
Louisiana Transportation Research Center

Technical Assistance Report No. 13-02TA-P

**Assessment of Mitigating Transverse Joint Faulting on
Portland Cement Concrete Pavement with Polyurethane Foam on
LA 1 Bypass, State Project Number 034-30-0023**

by

Kevin Gaspard and Zhongjie Zhang

LTRC



4101 Gourrier Avenue | Baton Rouge, Louisiana 70808
(225) 767-9131 | (225) 767-9108 fax | www.ltrc.lsu.edu

TECHNICAL REPORT STANDARD PAGE

1. Report No. FHWA/LA.14/13-02-TA-P		2. Government Accession No.	3. Recipient's Catalog No.
4. Title and Subtitle Assessment of Mitigating Transverse Joint Faulting with Polyurethane Foam on LA 1 By Pass, State Project Number 034-30-0023		5. Report Date February 2015	
		6. Performing Organization Code LTRC Project Number: 13-02TA-P State Project Number: 034-30-0023	
7. Author(s) Kevin Gaspard and Zhongjie Zhang		8. Performing Organization Report No.	
9. Performing Organization Name and Address Louisiana Transportation Research Center 4101 Gourrier Avenue Baton Rouge, LA 70808		10. Work Unit No.	
		11. Contract or Grant No.	
12. Sponsoring Agency Name and Address Louisiana Department of Transportation and Development P.O. Box 94245 Baton Rouge, LA 70804-9245		13. Type of Report and Period Covered Technical Assistance October 2007 to February 2012	
		14. Sponsoring Agency Code	
15. Supplementary Notes Conducted in Cooperation with the U.S. Department of Transportation, Federal Highway Administration			
16. Abstract <p>A case study was conducted by the Louisiana Transportation Research Center (LTRC) to assess the effectiveness of reducing faulting on jointed concrete pavement (JCP) with polyurethane foam (PF) on LA 1 Bypass, S.P. 034-30-0023. The PF fault correction process entailed reducing faults to approximately 0.25 inches by saw cutting full depth through the joints and lifting the slabs with PF whose free rise density was 6 pcf.</p> <p>A sampling plan was established where the entire project was measured for faulting and roughness by a high speed profiler before treatment with the PF fault correction process and 0.6, 2.1, 3.4, and 4.4 years after treatment. Three test sections with 11 slabs each were assessed with the falling weight deflectometer (FWD), ARRB walking profiler, and manual fault measurements. Seventeen cores were taken at various locations to obtain in-place PF samples. Statistical hypothesis testing was conducted comparing the density and strength of PF before and after it was injected into the pavement.</p> <p>Testing results indicated that repair goals of reducing faults were realized by the PF fault correction process, but at the sacrifice of severely reducing load transfer efficiency (LTE) at the transverse joints. Service life extensions of approximately 6.0 and 8.3 years on the north and south bound roadways, respectively, for fault height reduction were discovered. Unfortunately, the PF fault correction process severely impacted the LTE with 80 percent of joints having poor load transfer, 20 percent increase of joints needing load transfer improvement, and 0 percent of the joints in good condition. Deflections at the joints and center-intermediate slab locations were increased as much as 46 percent by the PF process indicating lower strength conditions. Void potentials were increased slightly (8 percent) by the process.</p> <p>The estimated service life extension based on the IRI parameter was 3.1 years and 5.7 years for the north and south bound roadways, respectively.</p> <p>Taking into account all the parameters analyzed in this study, the PF fault correction process was not recommended as a pavement preservation treatment for fault correction or ride quality improvement due to the detrimental effects discovered in this study.</p>			
17. Key Words polyurethane foam, transverse faulting, rehabilitation, jointed concrete pavement repairs, asset management, joint load transfer, roughness, profile, pavement preservation, Uretex, Nortex, concrete pavement restoration		18. Distribution Statement Unrestricted. This document is available through the National Technical Information Service, Springfield, VA 21161.	
19. Security Classif. (of this report)	20. Security Classif. (of this page)	21. No. of Pages	22. Price

**Assessment of Mitigating Transverse Joint Faulting on Portland Cement
Concrete Pavement with Polyurethane Foam on LA 1 Bypass, State Project
Number 034-30-0023**

by
Kevin Gaspard and Zhongjie Zhang

Louisiana Transportation Research Center
4101 Gourrier Avenue
Baton Rouge, LA 70808

Technical Assistance Report No. 13-02TA-P

conducted for

Louisiana Department of Transportation and Development
Louisiana Transportation Research Center

The contents of this report reflect the views of the author/principal investigator who is responsible for the facts and the accuracy of the data presented herein. The contents do not necessarily reflect the views or policies of the Louisiana Department of Transportation and Development or the Louisiana Transportation Research Center. This report does not constitute a standard, specification, or regulation.

February 2015

ABSTRACT

A case study was conducted by the Louisiana Transportation Research Center (LTRC) to assess the effectiveness of reducing faulting on jointed concrete pavement (JCP) with polyurethane foam (PF) on LA 1 Bypass, S.P. 034-30-0023. The PF fault correction process entailed reducing faults to approximately 0.25 inches by saw cutting full depth through the joints and lifting the slabs with PF whose free rise density was 6 pcf.

A sampling plan was established where the entire project was measured for faulting and roughness by a high speed profiler before treatment with the PF fault correction process and 0.6, 2.1, 3.4, and 4.4 years after treatment. Three test sections with 11 slabs each were assessed with the falling weight deflectometer (FWD), ARRB walking profiler, and manual fault measurements. Seventeen cores were taken at various locations to obtain in-place PF samples. Statistical hypothesis testing was conducted comparing the density and strength of PF before and after it was injected into the pavement.

Testing results indicated that repair goals of reducing faults were realized by the PF fault correction process, but at the sacrifice of severely reducing load transfer efficiency (LTE) at the transverse joints. Service life extensions of approximately 6.0 and 8.3 years on the north and south bound roadways, respectfully, for fault height reduction were discovered. Unfortunately, the PF fault correction process severely impacted the LTE with 80 percent of the joints having poor load transfer, 20 percent increase of joints needing load transfer improvement, and 0 percent of the joints in good condition. Deflections at the joints and center-intermediate slab locations were increased as much as 46 percent by the PF process indicating lower strength conditions. Void potentials were increased slightly (8 percent) by the process.

The estimated service life extension based on the IRI parameter was 3.1 years and 5.7 years for the north and south bound roadways, respectively.

Taking into account all the parameters analyzed in this study, the PF fault correction process was not recommended as a pavement preservation treatment for fault correction or ride quality improvement due to the detrimental effects discovered in this study.

ACKNOWLEDGEMENTS

The authors wish to thank DOTD and LTRC for providing the resources necessary for this project. The input from Uretek USA, Nortex Industries, NCFI Industries, and Bayer Systems was very helpful in capturing the properties of PF.

The authors would also like to extend a special thanks to the LTRC pavement unit staff, Mitch Terrell, Shawn Elisar, and Glen Gore.

IMPLEMENTATION STATEMENT

Taking into account all the parameters analyzed in this study, the PF fault correction process was not recommended as a pavement preservation treatment for fault correction or ride quality improvement. While fault reduction was achieved, it was at the sacrifice of joint load transfer efficiency and increased deflections in the slabs. Furthermore, ride quality was improved in the southbound roadway, but not the northbound roadway.

TABLE OF CONTENTS

ABSTRACT.....	iii
ACKNOWLEDGEMENTS.....	v
IMPLEMENTATION STATEMENT.....	vii
TABLE OF CONTENTS.....	ix
LIST OF TABLES.....	xii
LIST OF FIGURES.....	xiv
INTRODUCTION.....	1
OBJECTIVES.....	3
SCOPE.....	5
METHODOLOGY.....	7
Polyurethane Foam Material Properties.....	7
PF Fault Correction Process.....	10
Load Transfer Across Joints.....	11
Experiment Design.....	15
High Speed Profiler / Entire Roadway.....	16
Statistical Analysis.....	17
Selection of Test Section Locations and Assessments Conducted.....	18
FWD.....	18
ARRB Walking Profiler.....	20
Manual Fault Measurements.....	20
PF Samples.....	20
DISCUSSION OF RESULTS.....	23
IRI and Faulting Data Analysis, High Speed Profiler.....	23
IRI.....	23
Faulting.....	24
Test Section Assessments.....	26
FWD.....	26
ARRB Walking Profiler.....	29
Manual Joint Faulting Measurements.....	31
Laboratory Evaluation of PF Specimens.....	31
CONCLUSIONS.....	33
RECOMMENDATIONS.....	35
ACRONYMS, ABBREVIATIONS, AND SYMBOLS.....	37
REFERENCES.....	39
APPENDIX 1: LABORATORY EXPERIMENT.....	41

INTRODUCTION	41
Phase 1	41
Injection Molds	41
55 Gallon Barrel Test.....	42
Box Test	43
Sand Bucket Test	44
Phase 2	45
Laboratory Testing Results for Injection Mold Samples	45
Laboratory Testing for Barrel Specimens.....	49
Laboratory Testing for Box Specimens.....	53
Laboratory Testing for Sand Bucket Specimens	56
Groupings of Test Data.....	57
Highlights From Experimental Program.....	60
APPENDIX 2: SPECIFICATIONS	62
APPENDIX 3: TEST SECTION LAYOUT.....	67

LIST OF TABLES

Table 1 PF expansion properties.....	10
Table 2 Parameters assessed by devices	16
Table 3 FHWA ride quality guide	17
Table 4 CPA fault height guide	17
Table 5 LTE table	19
Table 6 IRI statistical table (high speed profiler)	23
Table 7 Statistical table for faulting (high speed profiler).....	24
Table 8 LTE data for test sections	26
Table 9 Statistical results summary for deflections	28
Table 10 Statistical summary table for manual fault measurements	31
Table 11 Statistical summary table for PF parameters	32
Table 12 Density and UCS results from 3-in. mold specimens.....	46
Table 13 Density and UCS results for barrel test	51
Table 14 UCS and density test results from box test.....	54
Table 15 UCS and density results for sand/PF mixture.....	57

LIST OF FIGURES

Figure 1 Polyurethane foam properties.....	7
Figure 2 Polyurethane heterogeneous samples.....	8
Figure 3 Expansion/density/UCS.....	9
Figure 4 PF fault correction process.....	11
Figure 5 Normal joint.....	12
Figure 6 Faulted joint.....	13
Figure 7 Joint with full depth saw cut.....	14
Figure 8 Undersealed slabs.....	15
Figure 9 IRI versus years of service.....	18
Figure 10 Deflections vs. load.....	19
Figure 11 PF specimens.....	21
Figure 12 Regression graph (IRI vs. yrs.).....	24
Figure 13 Faulting vs. years for northbound roadway.....	25
Figure 14 Faulting vs. years (southbound roadway).....	25
Figure 15 Void potential test section 1.....	27
Figure 16 Void potential for test section 2.....	27
Figure 17 Void potential for test section 3.....	28
Figure 18 Profile and IRI for test section 1 (walking profiler).....	29
Figure 19 Profile and IRI for test section 2 (walking profiler).....	30
Figure 20 Profile and IRI for test section 3 (walking profiler).....	30
Figure 21 PVC injection molds.....	42
Figure 22 Barrel test.....	42
Figure 23 PF in barrel.....	43
Figure 24 Box test.....	43
Figure 25 Expanded PF in box.....	44
Figure 26 Sand bucket test.....	45
Figure 27 Specimens from 6-in. and 3- in. diameter molds.....	46
Figure 28 United testing machine.....	47
Figure 29 Load versus extension graphs.....	47
Figure 30 Specimens from barrel test.....	48
Figure 31 Drill and coring device.....	48
Figure 32 Cored barrel sample.....	49
Figure 33 Specimens from barrel test.....	49
Figure 34 Samples from box test.....	52
Figure 35 Sand/PF sample.....	55

Figure 36 Coring sand/PF bucket sample 55
Figure 37 Sand/PF specimens 56
Figure 38 Diagram of sand/PF mixture 56
Figure 39 UCS dry injection sample comparison 58
Figure 40 Density dry injection sample comparison 58
Figure 41 UCS wet injection sample comparison 59
Figure 42 Density wet injection sample comparison 59
Figure 43 UCS wet injection versus dry injection sample comparison 60
Figure 44 Density wet injection versus dry injection sample comparison 60

INTRODUCTION

In Louisiana, many of the older Portland Cement Concrete (PCC) pavements are in need of rehabilitation or replacement. The LA 1 Bypass in Natchitoches, La, was one such PCC pavement. It was over 32 years old with an average daily traffic of 15,800 with 20 percent trucks. It classifies as an urban principle arterial roadway. Its typical section consisted of a 9-in. thick PCC pavement with a 6-in. thick soil cement base course and asphaltic concrete shoulders. Supporting embankment of soils in the A-2-4 and A-4 according to the AASHTO group classifications were discovered. Star lugs were used as load transfer devices, and its transverse joint spacing was 20 feet [1]. It had faulting as high as 1 in. and international roughness index (IRI) values (in. \ mile) ranging from 150 to 450. The project was approximately 4 miles in length.

Several alternatives were investigated by DOTD District 08 to address the poor ride quality and severe faulting on this project. The estimated construction costs for their top four alternates were as follows:

1. Reconstruction	\$9.0 million
2. Rubblize & AC overlay	\$3.5 million
3. Patch/level/AC overlay	\$3.0 million
4. Level with PF	\$1.3 million

Available funding for this project was \$2.2 million. On a previous project, DOTD District 08 conducted a repair experiment where faulting was reduced on several PCC pavement slabs by saw-cutting full depth through the joints and injecting polyurethane foam (PF) into the pavement structure. Replacing entire slabs or full depth patches at joints is costly and can require lane closures for days or weeks. The advantage of the PF fault correction process is that traffic can be placed on the treated area within 15 minutes, making it an excellent choice for a quick repair method. According to the district, based upon visual inspection, the slabs on that project appeared to be performing well.

The Louisiana Transportation Research Center (LTRC) was commissioned to assess the PF fault correction process and compose a report on its performance after monitoring it for a period of approximately five years.

OBJECTIVES

The primary objective of this research was to evaluate the Uretek Method of correcting transverse joint faulting with polyurethane foam (PF) on the La 1 Bypass for a period of approximately 5 years. This was accomplished using the high speed profiler, walking profiler, Falling Weight Deflectometer (FWD), manual fault measurements, and laboratory tests on PF.

SCOPE

The high speed profiler was used to collect IRI (in./mile) and faulting data before treatment on the entire project and was used as the control for the statistical analysis. Subsequent assessments after the fault correction process took place were at 0.6, 2.1, 3.4, and 4.4 years on the entire project.

Ten joints on 11 adjacent slabs were selected at three locations on the project. The locations were selected based upon finding a group of adjacent slabs with faulting in excess of 0.25 inches so the impact of the PF fault correction process could be assessed. Additionally, all slabs in the groups did not have distresses such as transverse or longitudinal cracks.

The three test sections (11 slabs each) were each assessed before and after the fault correction process with the Falling Weight Deflectometer (FWD), AARB walking profiler, and manual fault measurements. The FWD tests were performed 6 inches before and after each joint as well as every 5 feet longitudinally on the slab in the right wheel path. The walking profiler and manual fault measurements were also taken on the right wheel path before and after the fault correction process.

In order to determine the difference in density and strength in the PF between its free rise state (no confining pressure during curing) and its confined state (injected beneath the slab), samples were taken. Thirty free rise samples were obtained by injecting the PF into 3-in. diameter x 3- in. height molds. In-place PF specimens were obtained by coring through the concrete and base course. Unconfined compression testing and density testing was conducted in accordance with ASTM D 1621 and D 1622.

METHODOLOGY

Polyurethane Foam Material Properties

Polyurethane is any polymer consisting of a chain of organic units joined by urethane links as shown in Figure 1a. Polyurethane polymers are formed by a monomer containing at least two isocyanate functional groups reacting with another monomer containing at least two alcohol groups in the presence of a catalyst [2-8].

Polyurethane foam (PF) is polyurethane modified by reacting an isocyanate group with a blowing agent such as a hydroxyl group, hydrofluorocarbons (HFC), liquid carbon dioxide, or acetone as shown in Figures 1b and 1c [2-8].

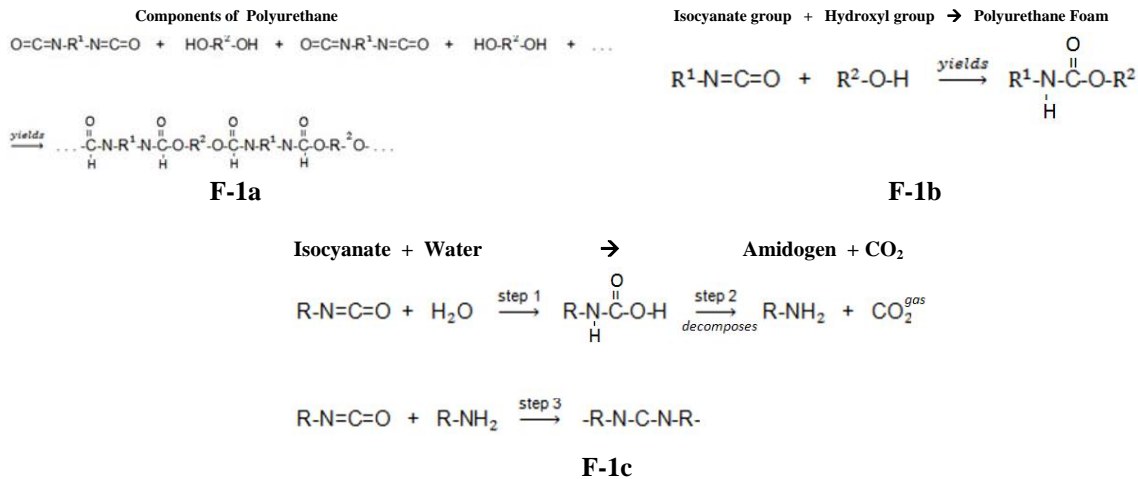


Figure 1
Polyurethane foam properties

PFs can be either hydrophilic or hydrophobic. Hydrophilic PF properties allow it to unite with or dissolve in (gaseous or liquid) water; whereas, a hydrophobic PF resists uniting with or dissolving in gaseous or liquid water [2-4]. Hydrophobic PF should be specified for pavement applications since liquid water may be present in voids. The term *hydrophobic* can be misleading, though, as it does not mean the PF is waterproof, water resistant, or that it will retain its structural properties when injected into liquid water.

LTRC conducted a laboratory experiment in conjunction with Uretek USA and Bayer Industries to capture the properties of hydrophobic PF when injected into dry and wet environments in July 2007. Appendix 1 presents a brief description of the experiment along

with the results. That research indicated that the hydrophobic PF parameters of density and strength were severely impacted when injected into liquid water.

Injecting PF into a void can cause the material to have both varying layers of density and strength as shown in Figure 2a. Practically speaking, injecting PF into a highway pavement structure produces a heterogeneous material [7-8]. Highway pavement conditions typically provide both free rise and confining conditions. *Free rise* refers to allowing the PF to expand with minimal confinement [2-5]. As shown in Figure 2b, when a PF is allowed to expand without confinement it will split and fracture, adversely impacting its strength and density. *Confinement* refers to conditions that provide restraining forces to retard the expansion of the PF. The density and strength of the PF should increase when confining forces are present [2-5]. For instance, consider the situation where PF is injected into a void that is 2 in. deep beneath a concrete slab. As the PF begins its expansion, the first 2 in. will be free rise conditions since confining pressures are not present during this time. Once the PF contacts the concrete slab and begins to lift it, confining pressures should begin to affect the PF density and strength. These confining pressures may differ during the lifting process depending upon conditions such as slab stiffness, load transfer efficiency at the joints, slab thickness, and the profile geometry of the slab [7-8].

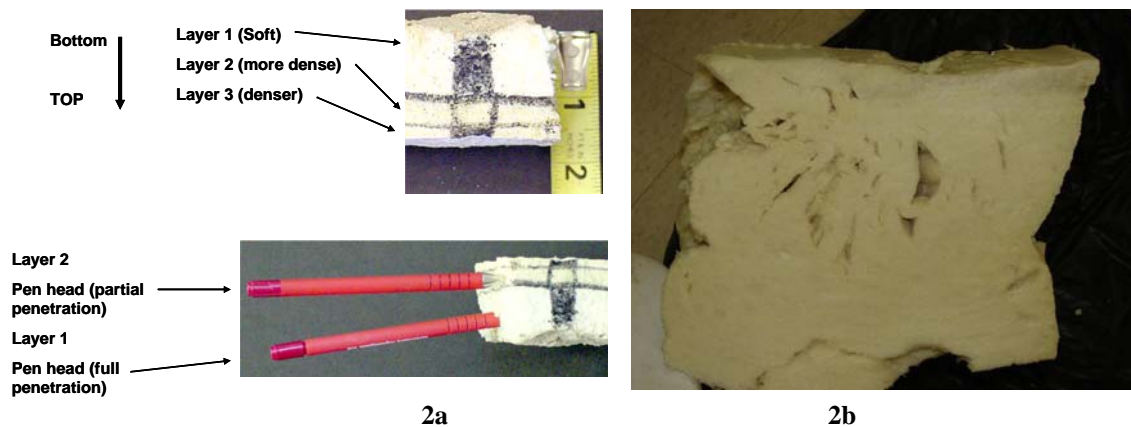


Figure 2
Polyurethane heterogeneous samples

The relationship of unconfined compressive strength at ultimate load, density, and expansion characteristics for PF are presented in Figure 3. As PF expansion increases, its density decreases. Conversely, unconfined compressive strength (UCS) increases as density increases. The density of polyurethane is approximately 72 lbs. per cubic foot (pcf). The expansion of polyurethane into a PF is calculated by dividing the density of polyurethane by the desired density of polyurethane foam. For example, 72 pcf divided by 4 pcf corresponds

to an expansion of 18.

Table 1 presents the increase in PF material that is required to fill equivalent volumes relative to a PF with a density of 4 pcf, under free rise conditions (no confinement). For example, it takes 33.3 percent more material for a 6 pcf PF to fill the same volume as a 4 pcf PF, based upon its expansion factor. In terms of cost, that would also mean that it could cost 33.3 percent more to use a 6 pcf PF than a 4 pcf PF based upon expansion factors in “free rise” conditions.

The target PF free rise density and unconfined compressive strength (UCS) specified on this project were 6 pcf and 100 psi, respectively. Currently, DOTD specifies a PF with a density range of 3 to 4 pcf and a minimum UCS of 50 psi as presented in Appendix 2.

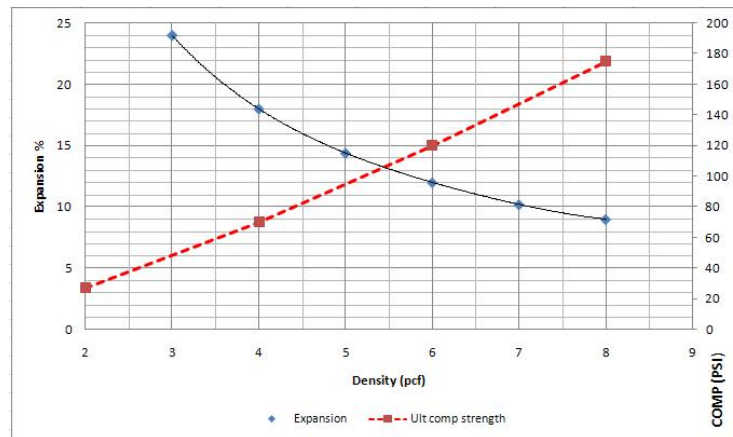


Figure 3
Expansion/density/UCS

Table 1
PF expansion properties

PF (pcf)	(1) Expansion factor from 72 pcf	(1) Percent increase relative to 4 pcf
4.0	18.0	0.0
5.0	14.4	20.0
6.0	12.0	33.3
7.0	10.3	42.8
8.0	9.0	50.0
9.0	8.0	55.6
10.0	7.2	60.0
11.0	6.5	63.9
12.0	6.0	66.7
(1) Free rise conditions		

PF Fault Correction Process

While faults contribute to the reduction of ride quality as measured by the IRI, they are by no means the sole source of poor ride quality. So reducing faulting on a roadway may or may not improve ride quality to an acceptable criteria as established by an agency. Ride quality on PCC roadways can be attributed to many factors such as cracking, pavement profile, joint spacing, joint width, and faulting.

According to the PF contractor (Uretek USA) on this project, faults cannot be reduced consistently to less than 0.25 in., and roadway profile adjustments on long sections of roadway cannot be achieved, as well [7][8]. Therefore, fault height reduction to 0.25 in., not elimination, was the outcome of this project. Figure 4 presents (generally) the PF fault correction process. The PF fault correction process has five major steps that can vary slightly based upon which PF contractor is awarded the project as well as roadway types (2 lane, 4 lane, 6 lane, etc.)/[8]:

1. Identify the joint to be treated.
2. Saw cut full depth through the joint.
3. Place devices at the joint to monitor the fault height and on the slab to monitor changes in its vertical displacement.

4. Drill holes through the slab and base course in intervals (typically 4 to 6 ft.) (longitudinal and transverse) determined by the PF contractor and/or project specifications.
5. Inject PF material through the holes and simultaneously monitor both changes in the fault height and vertical displacement of the slab. Once the desired fault height (0.25 in.) is reached, stop injecting PF near the joint. PF is then injected at additional slab locations until 1 mm of vertical movement is measured. This is called undersealing and its purpose is to fill any voids that may have been created beneath the slab by lifting the joints to minimize the fault.



Figure 4
PF fault correction process

Load Transfer across Joints

When a concrete slab is new, there should be no faulting at the joints (see Figure 5). Support at the joints, usually measured by load transfer efficiency (LTE), is the summation of support from the subgrade (X1), support from the base course (X2), aggregate interlock between the

slabs (X3), and the dowel bar(s) or star lugs, hereafter referred to as dowel bars (X4) as presented in Figure 5 [9-11].

$$LTE = X1 + X2 + X3 + X4 \quad (1)$$

Support from the subgrade (X1) and base course (X2) can be represented in terms of their dynamic modulus whereas the support from the aggregate interlock (X3) and dowel bars (X4) can be represented by their corresponding shear strengths.

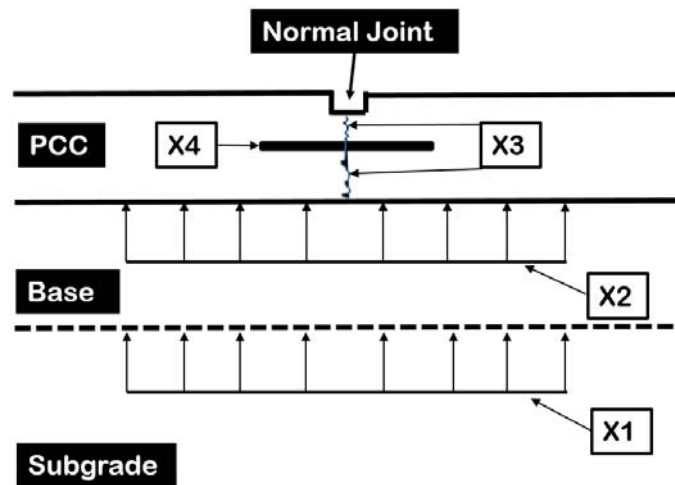


Figure 5
Normal joint

While in service, factors such as traffic loading, seasonal temperature and moisture fluctuations, base course erosion, subgrade erosion, and dowel bar failures lead to faulting at the joints as presented in Figure 6 [9-11].

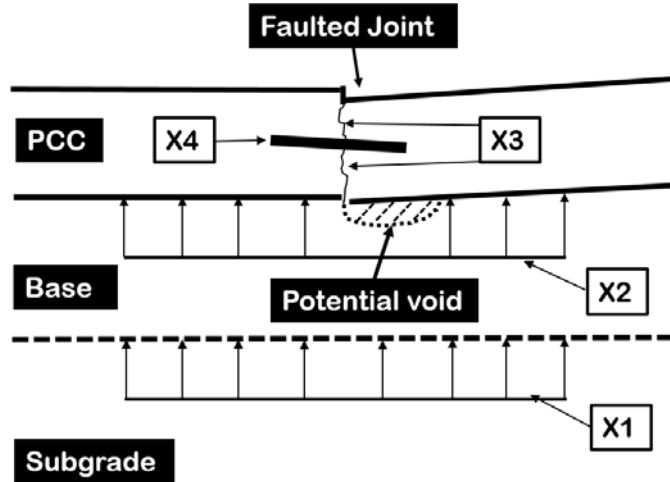


Figure 6
Faulted joint

There are two primary scenarios that may occur during the PF fault correction process. Scenario 1 is when the slabs lock together during the lifting process. When this occurs, fault height reduction is no longer possible at that location. This creates an issue since the maximum fault height reduction cannot be achieved at that location. For example, say the fault height between two slabs was originally 1.5 in. The PF fault reduction process begins and the slabs lock together when the fault height is 0.75 in. In this case, the maximum fault reduction to 0.25 in. cannot occur.

Scenario 2 differs from Scenario 1 in that full depth saw cuts are performed through the joints prior to the PF fault correction process as presented in Figure 7. From there, the PF fault correction process continues uninhibited until the faulting is reduced to at least 0.25 in. On this project, full depth saw cuts were performed at all joints.

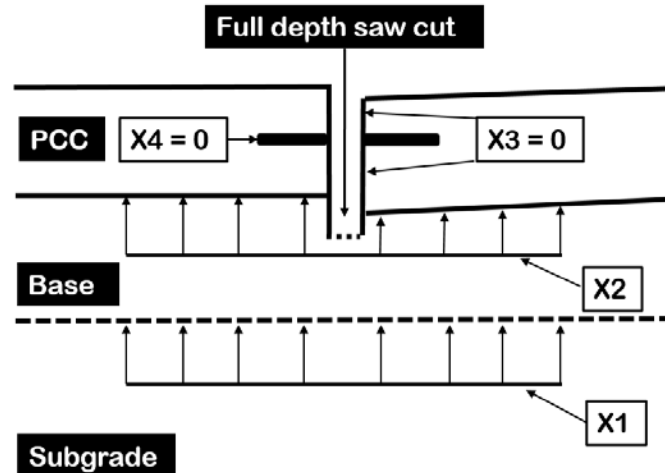


Figure 7
Joint with full depth saw cut

During the PF fault reduction process, LTE at the joint is severely reduced due to several factors. First, the full depth saw cut completely eliminates whatever support was available from aggregate interlock (X3) and the dowel bars (X4). Second, PF has a lower dynamic modulus than the subgrade and base course [6-8]. Therefore, once PF is injected into the subgrade, it can expand not only into the subgrade, but also into the base course and voids beneath the PCC slab [7][8]. The addition of PF into the subgrade/base course/void matrix, effectively reduces the support (X1 & X2) thus contributing to a loss in LTE [7][8]. So after the PF fault correction process, LTE is equal to the sum of subgrade-PF (X1) and base course-PF (X2) moduli, with (X1 + X2) after treatment being less than (X1 + X2) before treatment due to the incorporation of PF.

$$\text{LTE (after treatment)} = X1 + X2 \quad (2)$$

As described previously, the PCC slabs are undersealed with PF once fault reduction has taken place to fill any voids that may have developed by lifting the slab joints as presented in Figure 8 [7][8]. On a previous project, the thickness of the PF underseal layer was approximately 0.25 in. [7]. The undersealing process also changes the support stiffness characteristics by incorporating PF into the subgrade (X1) and base course (X2), thereby reducing their dynamic moduli. Because of that, deflection measurements taken on the slab or its joints after the PF undersealing process are generally larger than deflections prior to the process [7][8].

Future rehabilitation methods may be limited by this process. With the alteration of slab support (more elastic due to PF) and increased deflections, major rehabilitation options such

as rubblization and pavement replacement in conjunction with base course and subgrade restabilization may be prohibited. Regarding rubblization, the change in dynamic modulus of the base course and subgrade brought about by the increased “bounce” from PF may inhibit the fracturing of the pavement with resonant frequency breakers, multihead breakers, or guillotine devices. Restabilization of the base course and subgrade may also be prohibited because PF may not break up into small pieces with current pulverization devices. Large pieces of PF would interfere with cementitious stabilization of the soil or base course and create weak spots within the cement-soil-PF matrix. If that were the case, then the base course-subgrade-PF zone would have to be completely removed and replaced with select soils, which in turn, could be stabilized with cement. In either case, major issues due to the presence of PF in the subgrade or base course manifest in regards to future rehabilitation treatment selection.

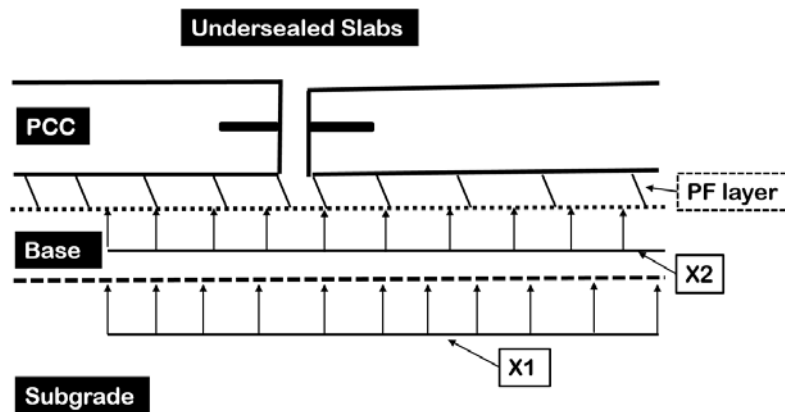


Figure 8
Undersealed slabs

Experiment Design

The experiment consisted of conducting tests with the high speed profiler, walking profiler, FWD, manual fault measurements, and laboratory tests before and after the PF fault correction process as presented in Table 2. The high speed profiler was the only device used to assess the entire project in both directions. Details of testing are provided in the following text.

Table 2
Parameters assessed by devices

Device/ Method	Location	Parameter
High speed profiler	Entire project	(1) IRI (2) Faulting
Walking Profiler	Test sections	(1) Profile (2) IRI
FWD	Test sections	(1) Voids (2) Load transfer efficiency (3) Deflections
Manual fault measurements	Test sections	(1) Faulting
Laboratory tests	Random sections	(1) Unconfined compressive strength (2) Density

High Speed Profiler/Entire Roadway

The high speed profiler was used to collect IRI (in.\ mile) and faulting data before treatment on the entire project and was used as the control for the statistical analysis. Subsequent assessments after the PF fault correction process took place were conducted at 0.6, 2.1, 3.4, and 4.4 years on the entire project. The outside travel lanes in both directions were tested before and after treatment. The IRI was reported in 0.1 mile intervals and faults were tabulated as the number of faults greater than 0.25 in. per 0.1 mile. Faulting was reported in this way since the purpose of the project was to reduce faulting to 0.25 in., not eliminate it. Additionally, results from the high speed profiler fault measurements can be biased if faulting less than 0.25 in. is specified in the data processing software because the algorithm can “confuse” surface cracks with joint faulting.

According to FHWA, the IRI limits presented in Table 3 can be used to define ride quality [12]. Though the purpose of the project was not to reduce the IRI to a specific level, IRI measurements after the PF fault correction process were compared to the results in Table 3 to categorize the ride quality. The Concrete Paving Association published roughness guidelines for fault heights as presented in Table 4 [13]. Based on their guidelines, fault heights should be less than 1/32 in. in order to minimize the contribution of faulting to roadway roughness.

Table 3
FHWA ride quality guide

Ride Quality	IRI (in. per mile)
Smooth	0 to 80
Moderate	80 to 130
Rough	>130

Table 4
CPA fault height guide

Average fault (in.)	Faulting index	Comments
1/32 (0.0312)	5	No roughness
1/16 (0.0625)	10	Minor faulting
3/32 (0.0936)	15	Trigger grinding needed
1/8 (0.1250)	20	Expedite project
5/32 (0.1563)	25	
3/16 (0.1875)	30	Discomfort begins
7/32 (0.2188)	35	
1/4 (0.2500)	40	Immediate attention required
Table from Technical bulletin (TB-008.0 CPR ,1990), Concrete Paving Technology		

Statistical Analysis

Two methods were employed to analyze the IRI and faulting data from the high speed profiler. An analysis of variance (ANOVA) was conducted to compare the control (before treatment) to the time series (0.6, 2.1, 3.4, and 4.4 years) after treatment conditions to determine if significant differences existed at alpha = 0.05 using Tukey-Kramer adjustments [14].

The service life of a treatment was determined from the point of intersection between the initial roadway condition (before treatment) with the after treatment regression line as presented in Figure 9. For example, the intersection of the after treatment regression line with the before treatment (initial condition) IRI value “200” occurred at occurred at 2.8 years. Therefore, the service life of the treatment was 2.8 years.

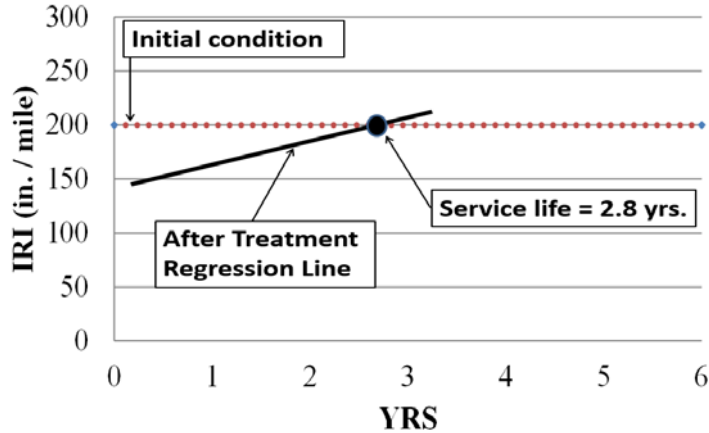


Figure 9
IRI versus years of service

Selection of Test Section Locations and Assessments Conducted

Ten joints on 11 adjacent slabs were selected at three locations on the project as presented in Appendix 3. The locations were selected based upon finding a group of adjacent slabs with faulting in excess of 0.25 in. so the impact of the PF fault correction process could be assessed. Additionally, all slabs in the groups were free of visible distresses such as transverse or longitudinal cracks.

The three test sections (11 slabs each) were each assessed before and after the PF fault correction process with the Falling Weight Deflectometer (FWD), AARB walking profiler, and manual fault measurements. The FWD tests were performed 6 in. before and after each joint as well as every 5 ft. longitudinally on the slab in the right wheel path. The walking profiler and manual fault measurements were also taken on the right wheel path before and after the fault correction process. Base lines were painted on the pavement with test points marked to ensure testing was conducted at similar locations before and after the fault correction process. Table 2 summarizes the parameters evaluated with each device.

FWD

The FWD was used to measure LTE at the joints, void potential beneath the slab, and deflections. Loads of 9,000, 12,000, and 16,000 lbs. were used at each test point with three drops at each load. Testing was conducted between the months of January and April.

According to FHWA and other sources, load transfer efficiency (LTE) can be categorized into three groups, as shown in Table 5 [9-11,15]. It was postulated that the LTE would be

severely impacted by the fault correction process since every joint had to be saw cut full depth in order to correct faulting with the PF process. Full depth saw cutting through joints removed load transfer contributions from the load transfer devices and aggregate interlock as presented in Figure 7.

Table 5
LTE table

Load transfer efficiency	Condition
LTE \geq 80 %	Good
80% < LTE \leq 60 %	Fair (may need improvement)
LTE < 60 %	Poor (needs improvement)

Void potential or loss of subgrade support, hereafter referenced as void potential was determined by plotting the deflections of the first sensor versus load and determining the Y intercept as presented in Figure 10 [7], [16-18]. According to the AASHTO 1993 Pavement Design Guide, a Y intercept value greater than 0.002 in. (2 mils) represents either a void or a loss of support [16]. In a previous study conducted by LTRC, the void potential method was validated with coring [7].

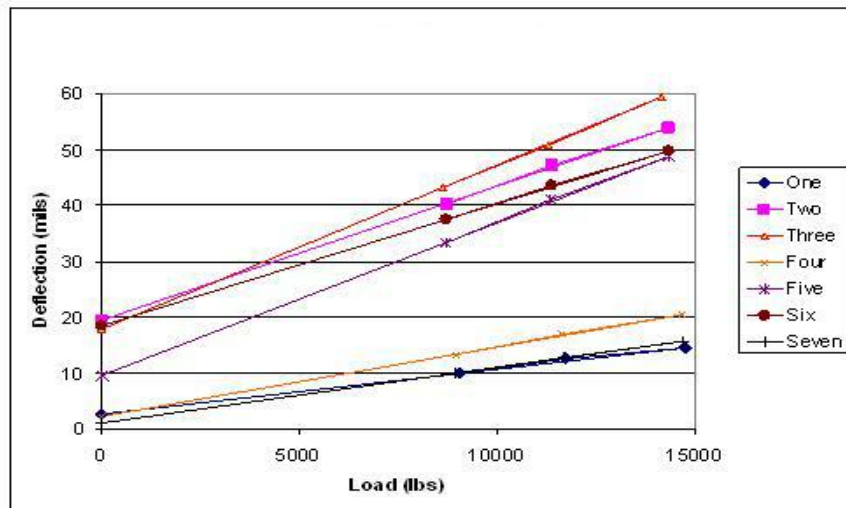


Figure 10
Deflections vs. load

The deflections (mils) from the first sensor were statistically analyzed with an ANOVA to compare the deflections between the before and after treatments for two groups: deflections at joints and deflections at center and intermediate points on the slab. In a previous study, LTRC found that PF injections either generally maintain deflections or increase them [7]. Maintaining deflections indicates no improvement and increasing deflections indicate worsening conditions.

ARRB Walking Profiler

The profile and IRI were measured before and after the fault correction process with this device. Footworks, a proprietary software program developed by ARRB was used to determine the IRI from the walking profiler measurements [19].

Manual Fault Measurements

Faults were measured before and after the fault correction process with a straight edge and tape. An ANOVA was conducted to determine if statistical differences occurred before and after treatment.

PF Samples

The density and strength of polyurethane foam is influenced by the confining pressure present when it is expanding/curing. In order to determine the difference in density and strength in the PF between its free rise state (no confining pressure during curing) and its confined state (injected beneath the slab), samples were taken. Thirty free rise samples were obtained by injecting the PF into 3-in. diameter x 3-in. height molds. The PF was allowed to expand inside the mold with no confining pressure as shown in Figure 11a. In-place PF specimens were obtained by coring through the concrete and base course as shown in Figure 11b. Though 17 cores were taken and the site was trenched in two locations, only eight usable PF specimens could be obtained from two cores. Unconfined compression testing and density testing were conducted in accordance with ASTM D 1621 and D 1622.

The parameters examined in the ANOVA statistical analysis (free rise versus in-place) were density, UCS at 3 percent strain and UCS at 10 percent strain, which is near ultimate load. The UCS at 3 percent strain is the parameter typically used to evaluate semi-rigid cement base courses in Louisiana.



Figure 11
PF specimens

DISCUSSION OF RESULTS

IRI and Faulting Data Analysis, High Speed Profiler

IRI

Profile measurements were taken on the entire project before treatment and 0.6, 2.1, 3.4, and 4.4 years after treatment with PF. As shown in Table 6, statistical differences did not occur on the northbound lanes. Though statistical differences were not discovered, with the exception of the measurement at year 4.4, a reduction in the average IRI values were discovered. The regression analysis revealed that the service life of the treatment was 3.1 years as presented in Figure 12a. Regarding the southbound lanes, statistical differences were present only at years 0.6, and 2.1 as presented in Table 6. The regression analysis revealed that the service life of the treatment was 5.6 years as presented in Figure 12b. The IRI measurements in both directions did not produce a smooth to moderate IRI (80 to 130), as presented in Table 3.

In a study conducted by the Michigan Department of Transportation (MDOT), the estimated service life of load transfer efficiency, ride quality improvement, and base support was approximately one year [20].

Table 6
IRI statistical table (high speed profiler)

NB IRI Group	Control	0.6 yrs.	2.1 yrs.	3.4 yrs.	4.4 yrs.	Adjusted P-value	Statistical Hypothesis Test	Similar or Different
Mean	250.50	216.45	238.84	249.29	270.60			
STDEV	53.5801	59.3284	46.8320	48.1671	44.9659			
n	32	32	32	32	32			
Test 1						<.0001	F	Different
Test 2						0.19	Tukey-Kramer	Similar
Test 3						0.99	Tukey-Kramer	Similar
Test 4						1.00	Tukey-Kramer	Similar
Test 5						0.86	Tukey-Kramer	Similar
SB IRI Group	Control	0.6 yrs.	2.1 yrs.	3.4 yrs.	4.4 yrs.	Adjusted P-value	Statistical Hypothesis Test	Similar or Different
Mean	276.37	219.60	237.35	249.56	263.66			
STDEV	57.3926	44.7683	49.1257	54.6701	48.9062			
n	39	39	39	38	39			
Test 1						<.0001	F	Different
Test 2						<.0001	Tukey-Kramer	Different
Test 3						0.0278	Tukey-Kramer	Different
Test 4						0.3881	Tukey-Kramer	Similar
Test 5						0.9845	Tukey-Kramer	Similar

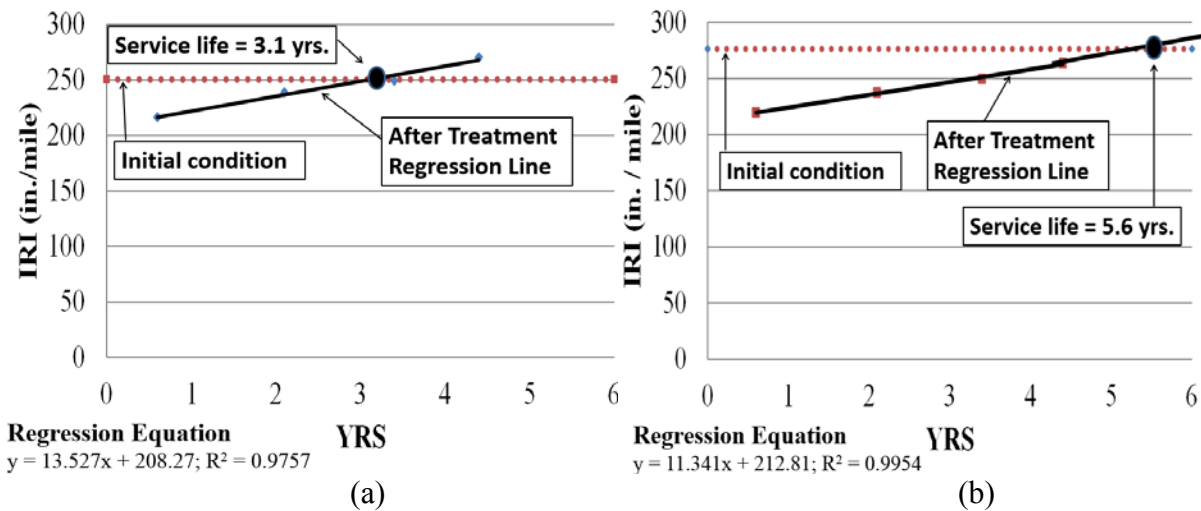


Figure 12
12(a) Northbound IRI regression graph, 12(b) Southbound IRI regression graph

Faulting

As shown in Table 7, a statistical difference exists between the before and after treatment data sets at years 0.6, 2.1, 3.4, and 4.4 for both the north- and southbound lanes indicating that improvements existed beyond 4.4 years. A regression analysis was performed for the north- and southbound lanes, as presented in Figures 13 and 14. The results indicated that the treatments had service lives of 6.04 and 8.32 years for the north- and southbound lanes, respectively.

Table 7
Statistical table for faulting (high speed profiler)

NB Faulting Group	Control	0.6 yrs.	2.1 yrs.	3.4 yrs.	4.4 yrs.	Adjusted P-value	Statistical Hypothesis Test	Similar or Different
Mean	10.28	2.40	3.06	4.88	6.81			
STDEV	6.4419	3.2908	2.6388	3.1392	3.8222			
n	32	32	32	32	32			
Test 1						<.0001	F	Different
Test 2						<.0001	Tukey-Kramer	Different
Test 3						<.0001	Tukey-Kramer	Different
Test 4						0.0226	Tukey-Kramer	Different
Test 5						0.0011	Tukey-Kramer	Different
SB Faulting Group	Control	0.6 yrs.	2.1 yrs.	3.4 yrs.	4.4 yrs.	Adjusted P-value	Statistical Hypothesis Test	Similar or Different
Mean	14.38	2.67	3.38	4.45	6.5			
STDEV	6.0724	2.2633	2.8710	3.1597	4.3520			

n	39	39	39	39	39			
Test 1						<.0001	F	Different
Test 2						<.0001	Tukey-Kramer	Different
Test 3						<.0001	Tukey-Kramer	Different
Test 4						<.0001	Tukey-Kramer	Different
Test 5						<.0001	Tukey-Kramer	Different

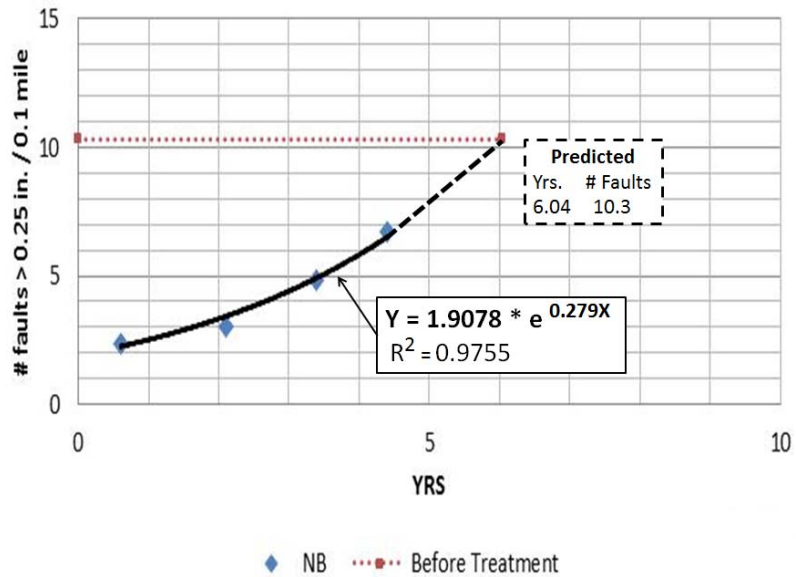


Figure 13
Faulting vs. years for northbound roadway

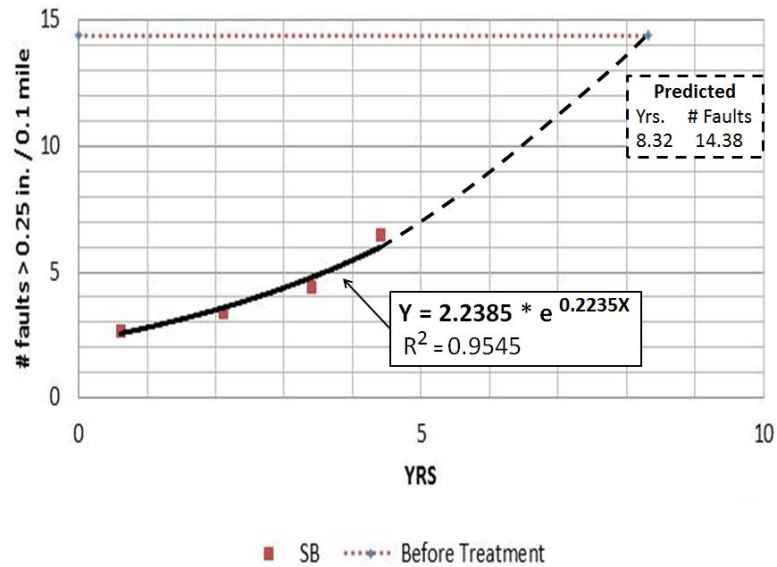


Figure 14
Faulting vs. years (southbound roadway)

Test Section Assessments

FWD

LTE. Table 8 presents the results of LTE readings before and after the fault correction process. The data clearly indicates that the process significantly reduced the LTE of the joints. Prior to injection, 26, 47, and 27 percent of the joints were in poor, fair, and good condition, respectively, and after injection, 80, 20, and 0 percent of the joints were in poor, fair, and good condition, respectively. This severe reduction in LTE was expected since every joint on the project had to be saw cut in order to reduce the faulting. In a previous study conducted by LTRC, PF was confirmed as not providing adequate support to improve LTE [7].

As previously mentioned, MDOT conducted a study using the Uretex method and it was determined that the estimated service life of load transfer efficiency, ride quality improvement, and base support was approximately one year [20]. Though not elaborated on in that study, it is believed that full depth saw cuts at the joints were not performed during the PF fault correction process, which may explain why they did not discover severe LTE reduction as measured in this study [20].

Table 8
LTE data for test sections

	Poor (needs improvement) LTE < 60%	Fair (may need improvement) 60% ≤ LTE < 80%	Good LTE ≥ 80%
% of joints Before	26	47	27
% of joints After	80	20	0
Percent change in category	+ 54	- 27	- 27
Note: A total of 30 joints were tested, 10 at each test section location			

Void Potential. Prior to the fault correction process, tested locations did not indicate a potential for voids, whereas 12 locations did after injection as presented in Figures 15 to 17. This indicates that the potential for voids was increased by approximately 8 percent by the process. This can be attributed to slab uplift movements caused by the fault correction process and issues with filling the voids beneath the slab during the undersealing process.

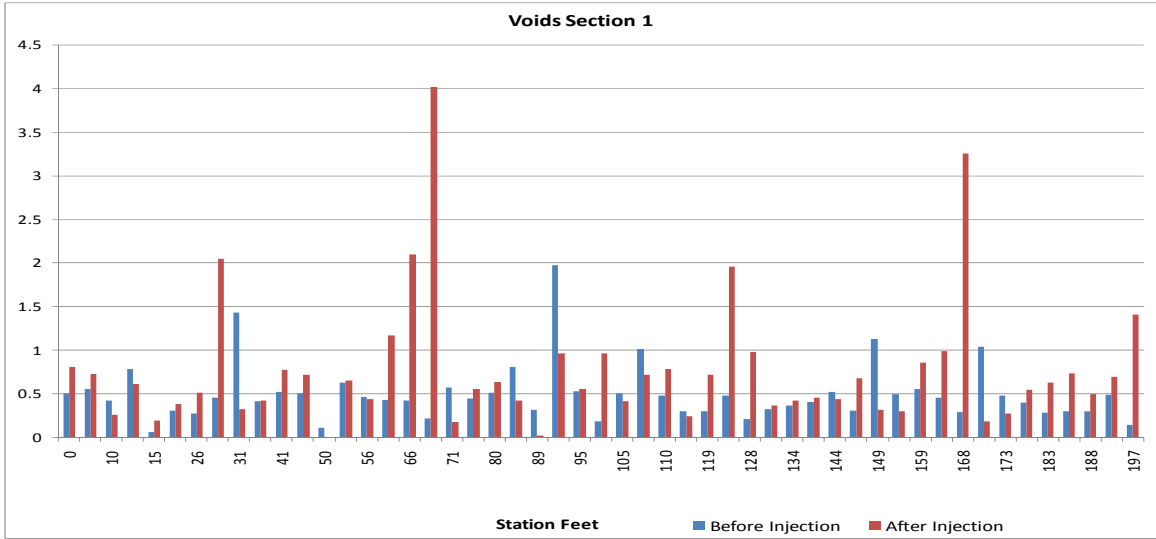


Figure 15
Void potential test section 1

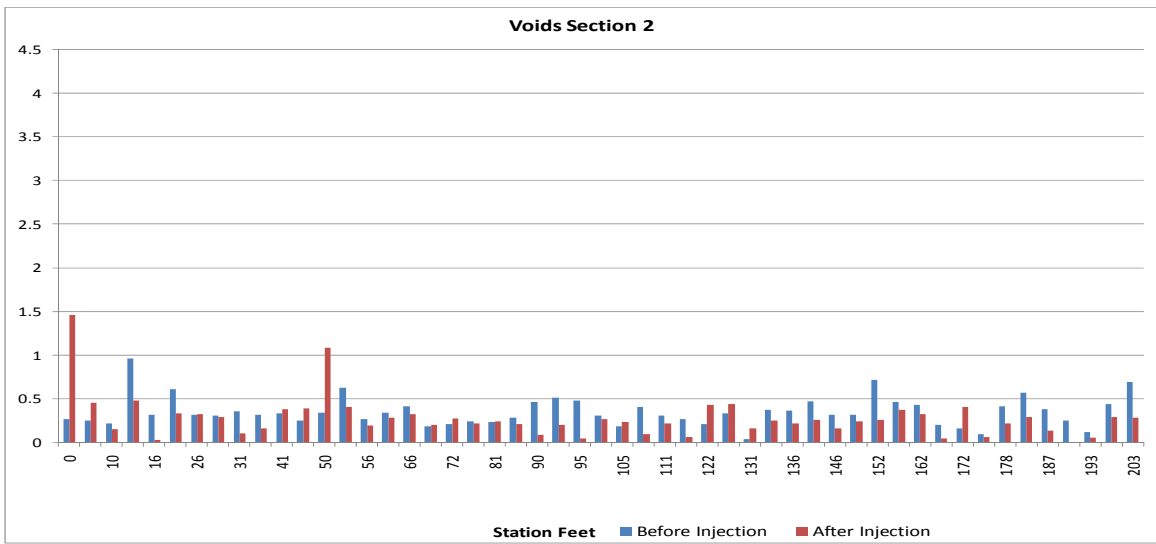


Figure 16
Void potential for test section 2

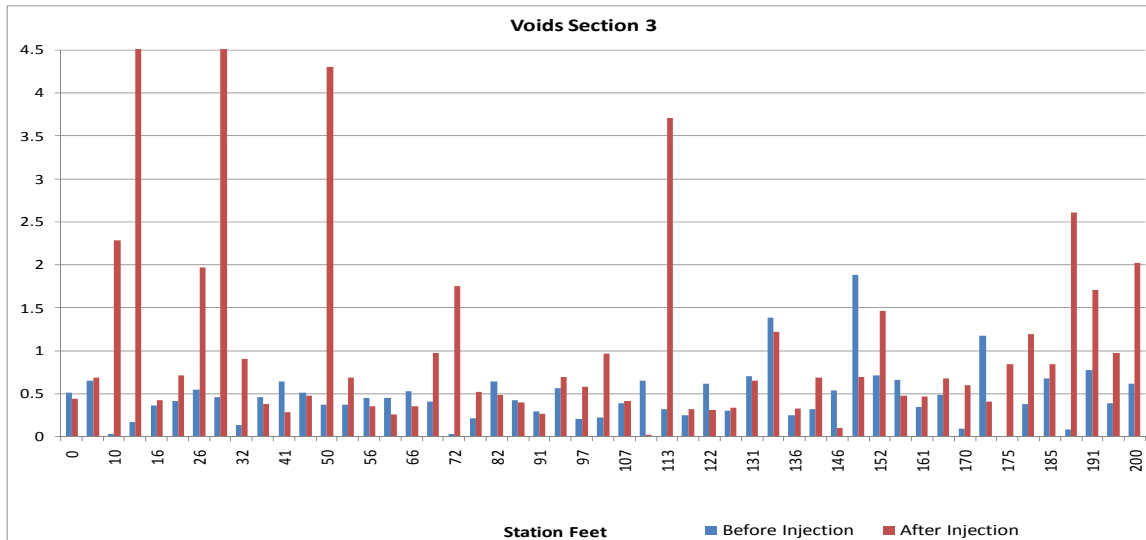


Figure 17
Void potential for test section 3

Deflections. Table 9 presents the statistical results comparing deflections before and after treatment for the joints and center-intermediate points. The results indicated that a significant difference exists at both the joints and center-intermediate points with the deflections being increased as much as 46 percent after treatment. This was consistent with research previously conducted by LTRC and MDOT [7-8][20].

Table 9
Statistical results summary for deflections

Parameter	Before	After	Adjusted (2) p-value	Comments
Deflections (1) (Joints)				
Mean	8.121 mils	11.912 mils	p<0.0001	Statistically different
STDEV	1.4166	5.1517		
N	60	60		
Deflections (1) (Center & Intermediate Points)				
Mean	5.516 mils	7.750 mils	p<0.0001	Statistically different
STDEV	0.7912	2.7761		
N	93	93		
Legend: Mean = average; STDEV = Standard deviation; N = number of samples (1) 1 mil = 0.001 in. (2) Tukey-Kramer statistical hypothesis test				

ARRB Walking Profiler

Profile measurements and IRI readings were taken before and after fault corrections on the test sections as shown in Figures 18 to 20. Clearly, the figures illustrate the extreme slab roughness and excessive joint faulting were present before PF injection. The PF process did reduce faulting, but a “bumpy” profile was still present after PF injection. Improvements in ride quality, were realized by the process on the test sections as demonstrated by the reduction of the average IRI from 282 (before treatment) to 192 (after treatment) on the three test sections. However, as previously mentioned, the after treatment IRI did not produce a smooth to moderate (80 to 130) ride, as presented in Table 2. Unless the profile can be corrected during the PF fault correction and undersealing process, smooth or moderate ride quality cannot be obtained on roadways.

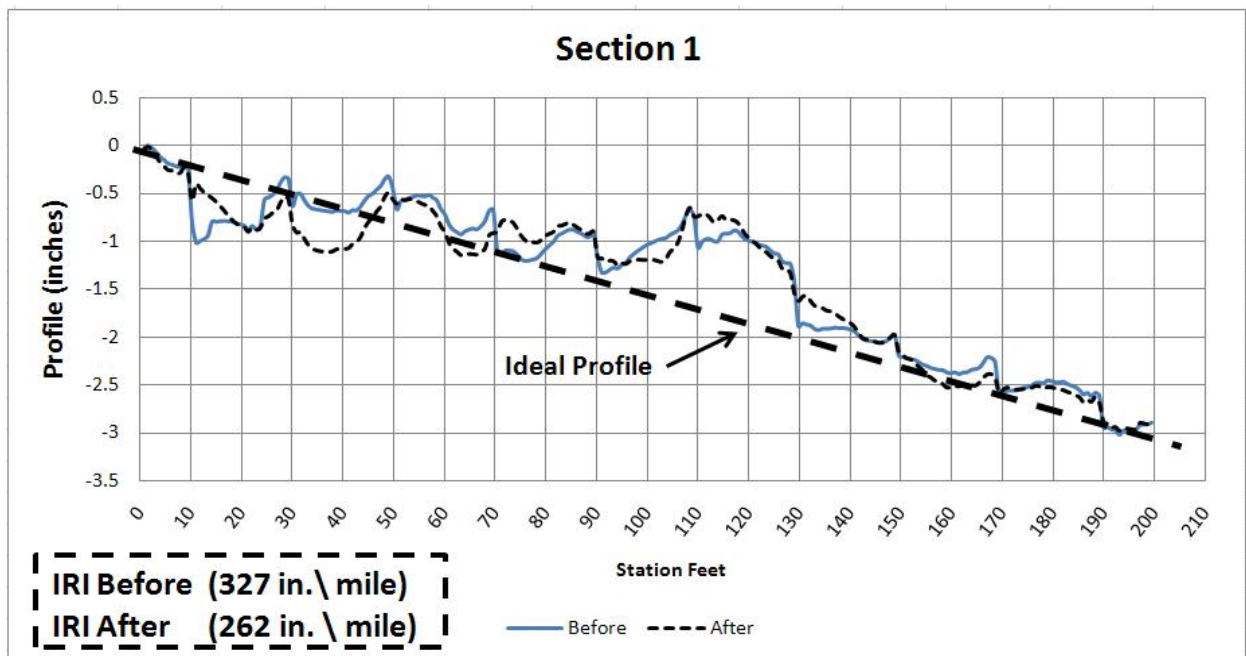


Figure 18
Profile and IRI for test section 1 (walking profiler)

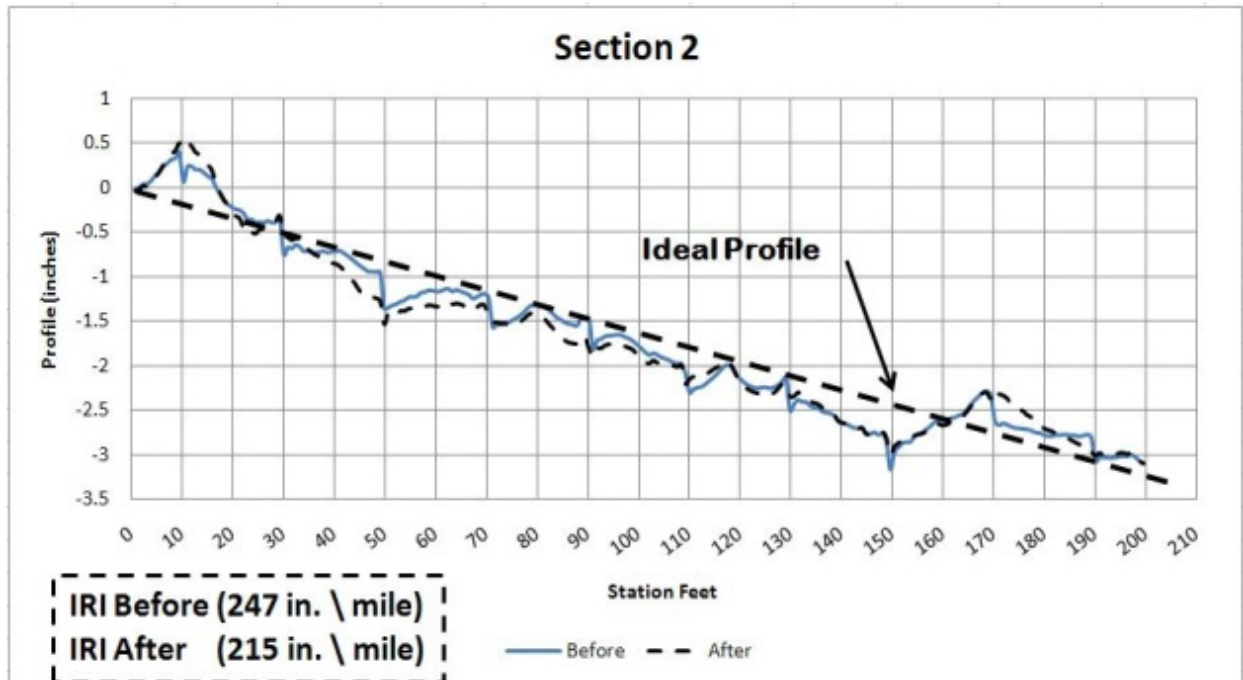


Figure 19
Profile and IRI for test section 2 (walking profiler)

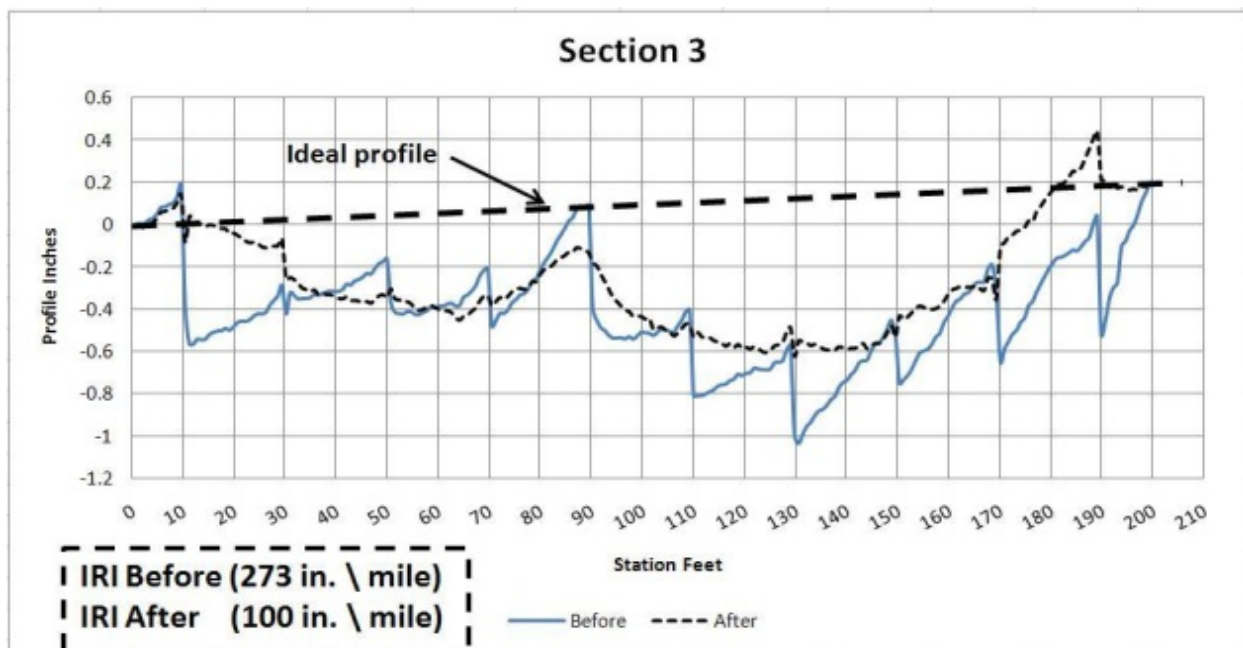


Figure 20
Profile and IRI for test section 3 (walking profiler)

Manual Joint Faulting Measurements

Measurements were taken at test sections 1 and 2 but were inadvertently not taken at test section 3. Statistical hypothesis testing was performed comparing the before and after measurements, and the results are presented in Table 10. A statistical difference exists between the before and after data sets with the mean height of faults value (0.105 in.) after injection being lower than the mean height of faults value (0.313 in.) before injection. This indicates an overall improvement in the reduction of fault heights.

Table 10
Statistical summary table for manual fault measurements

Parameter	Before	After	Adjusted (2) p-value	Comments
Manual faulting				
Mean	0.3125 in.	0.105 in.	p<0.0001	Statistically different
STDEV	0.1174	0.0766		
N	20	20		
Legend: Mean = average; STDEV = Standard deviation; N = number of samples (1) 1 mil = 0.001 in. (2) Tukey-Kramer statistical hypothesis test				

Laboratory Evaluation of PF Specimens

Table 11 presents statistical results from laboratory tests comparing free rise specimens to in-place specimens. Parameters addressed were density, UCS at 3 percent strain, and UCS at 10 percent strain, which is near ultimate load.

According to the statistical hypothesis test, a statistical difference exists for the density parameter. The mean in-place density (12.7 pcf) was higher than the mean free rise density (6.8 pcf). Conversely, a decrease and significant change in UCS was discovered. The mean in-place UCS at 3 percent strain (33.9 psi) was less than the mean free rise UCS (57.6 psi) and was statistically different. For the UCS at 10 percent strain parameter, the in-place UCS (99.1 psi) and free rise UCS (119.4 psi) were statistically different as well. The data infers that the confining pressures present while injecting the foam increased its density, and decreased its UCS at both 3 and 10 percent strain. In the experimental program outlined in Appendix 1, UCS strengths from simulated field conditions were less than free rise UCS strengths similar to what was discovered in this project. Reasons for this inconsistency of reduced strength in confined conditions and free rise specimens are unknown and warrant further research.

Table 11
Statistical summary table for PF parameters

Parameter	Free Rise	In-place	Adjusted (2) p- value	Comments
Density Mean STDEV N	6.798 pcf 0.3328 30	12.653 pcf 1.3659 8	p<0.0001	Statistically different
UCS @ 3% strain Mean STDEV N	57.602 psi 26.327 30	33.978 psi 13.793 8	p<0.0201	Statistically different
UCS @ 10% strain Mean STDEV N	119.41 psi 15.945 30	99.061 psi 31.316 8	p<0.0133	Statistically different
Legend: Mean = average; STDEV = Standard deviation; N = number of samples (1) 1 mil = 0.001 in. (2) Tukey-Kramer statistical hypothesis test				

CONCLUSIONS

The estimated service life extension based on the IRI parameter was 3.1 years and 5.7 years for the north and south bound roadways, respectively. Though the IRI was improved, a smooth to moderate ride (IRI range of 80 to 130) was not obtained. The primary reasons for the measured roadway roughness are:

1. The transverse joint faults were not reduced to 1/32 in. or less as recommended by the CPA.
2. The roadway profile was not corrected to its “as-built” grades.
3. The specifications did prescribe an IRI value per 0.1 mile section for the PF fault correction and undersealing process.

According to the PF contractor (Uretek USA) who performed the work on this project, the PF fault correction process cannot meet items 1 and 2 listed above and may be unable to meet item 3 depending upon the initial IRI (i.e., reducing an IRI from 450 to less than 130).

Reduction of fault heights to 0.25 in. was realized by the PF fault correction process, with service life extensions of approximately 6.0 and 8.3 years on the north and south bound roadways, respectfully.

Unfortunately, the PF fault correction process severely impacted the LTE with 80 percent of the joints having poor load transfer, 20 percent of the joints needing load transfer improvement, and 0 percent of the joints having good load transfer efficiency. It is reasonable to assume that this was primarily caused by saw cutting through the joints which completely eliminated LTE contributions from aggregate interlock and star lugs. Deflections at the joints and center-intermediate slab locations were increased as much as 46 percent by the PF process indicating lower strength conditions. Void potentials were increased slightly (8 percent) by the PF process.

The density of the PF was increased from approximately 6.8 to 12.7 pcf by injecting it beneath the slab. This was expected because confining conditions should increase its density in the absence of water. Conversely, this trend was not realized in the unconfined compressive strength tests. At 3 and 10 percent strains, the UCS were statistically different and lower in the confined conditions than in free rise conditions. Similar studies were not found in the literature search, so it is unknown if this is a typical trend.

DOTD can conserve funds by being attentive to these two characteristics of PF: expansion versus density and density/strength versus water sensitivity.

Higher density (i.e., 6 to 12 pcf) PF expands less and costs more to achieve similar results (void filling and slab lifting) than lower density (i.e., 3 to 4 pcf) PF. Therefore, DOTD should consider using a PF with a lower density (3 to 4 pcf) to conserve funds due to its expansion characteristics. DOTD has established performance specifications where both the density and UCS are specified for PF with penalties for being below or above specified limits as shown in Appendix 2.

Density/strength appears to be adversely impacted when PF is injected into locations where liquid water is present [7-8]. When the density/strength is reduced, it will compress more, thus requiring more material to be injected to fill the void and lift the slab, which in turn increases the cost.

RECOMMENDATIONS

The PF fault correction process should not be used as a pavement preservation treatment. It generally does not improve ride quality, does not eliminate faulting, severely reduces load transfer efficiency, and increases deflections at the joints and in the slab as well.

Furthermore, major rehabilitation processes such as rubblization and removal/replacement of the slab and base course restabilization may not be possible once this process has been used.

The PF fault correction process should only be used on short sections where a few adjacent slabs need fault corrections.

In order to obtain the best cost/benefit ratio, PF should be specified to have a density range of 3 to 4 pcf.

ACRONYMS, ABBREVIATIONS, AND SYMBOLS

ADT	Average Daily Traffic
FWD	Falling Weight Deflectometer
IRI	International Roughness Index
JCP	Jointed concrete pavement
DOTD	Louisiana Department of Transportation and Development
LTE	Load Transfer Efficiency
LTRC	Louisiana Transportation Research Center
pcf	pounds per cubic foot
PF	Polyurethane foam
UCS	Unconfined compressive strength

REFERENCES

1. Bolourchi, Z., Temple, W., and Shah, S., "Evaluation of Load Transfer Devices," Louisiana Department of Highways Research and Development Section, Research Report Number 97, November 1975.
2. Ashida, K., "Polyurethane and Related Foams: Chemistry and Technology," CRC; 1st Edition, September 2006
3. Oertel, G. "Polyurethane Handbook," New York: Macmillen Publishing Co., Inc., 1985 ISBN 0-02-948920-2.
4. Woods, G., "The ICI Polyurethanes Book," New York: John Wiley & Sons, Inc., 1990, ISBN 0-471-92658-2.
5. Sendijarevic V., Klempner, D., "Polymeric Foams And Foam Technology," Hanser Gardner Publications; 2nd edition, April 2004, ISBN-13: 978-1569903360
6. Kaushiva, B., "*Structure-Property Relationships of Flexible Polyurethane Foams*," Ph.D Thesis, Virginia Polytechnic Institute, August 1999.
7. Gaspard, K., and Morvant, M., "Assessment of the Uretek Process on Continuously Reinforced Concrete Pavement, Jointed Concrete Pavement, and Bridge Approach Slabs," Louisiana Transportation Research Center, Technical Assistant Report Number 03-2TA, December 2004.
8. Gaspard, K. and Zhang, Z., "Mitigating Tranverse Joint Faulting in Jointed Concrete Pavement with Polyurethane Foam," Transportation Research Record: Journal Of Transportation Research Board, Report Number 10-1637, pp 3-11, 2010.
9. Federal Highway Administration, Concrete Pavement Rehabilitation: Guide for Load Transfer Restoration, Publication FHWA SA-97-103. Washington DC, 1997.
10. National Highway Institute, Techniques for Pavement Rehabilitation, Training Course Materials, 1993
11. Synder, M., "Guide to Dowel Load Transfer Systems for Jointed Concrete Roadway Pavements," National Concrete Pavement Technology Center, Iowa State University, 2011.
12. Highway Performance Monitoring System, Appendix J, FHWA, USA, Department of Transportation, 1993.
13. Concrete Paving Technology (CPA), currently (ACPA), Technical Bulletin TB-008.0 CPR, 1990.

14. Devore, J., "Probability and Statistics for Engineering and the Sciences," Duxbury Press, 7th Edition, January 2007.
15. Button, J.W.; Lytton, R.L. "Guidelines for Using Geosynthetics with Hot Mix Asphalt Overlays to Reduce Reflective Cracking," *Journal of the Transportation Research Board*, 2004, Washington, D.C., 2007, pp. 111-119.
16. *AASHTO Guide for Design of Pavement Structures*, AASHTO, 1993.
17. Darter, M., Barenberg, E., Yrjanson, W., "Report 0077-5614," National Highway Research Program.
18. Crovetti, J., Deflection based Techniques for Jointed Concrete Pavement Systems," *Transportation Research Record* 1809, Paper 02-4029.
19. Footworks Software, ARRB, Broadway, Australia.
20. Opland, W. and Barnhart, "Evaluation of the Urettek Method for Pavement Undersealing," Research and Technology Section, Materials and Technology Division, Research Project Number 93 G-294, Research Report Number R-1340, August 1995.

APPENDIX 1: LABORATORY EXPERIMENT

INTRODUCTION

In July 2007, an experiment was conducted to capture the properties of Uretek 486 hydrophobic polyurethane foam (PF). This was accomplished through a two phase experiment. The first phase of the experiment consisted of injecting PF into dry and sometimes wet environments, described in detail later. Four injection environments were utilized, molds made from 3-in. and 6-in. diameter PVC pipe, a 55-gallon barrel, a box made from plywood and 2-in. by 4-in. wood, and a 5-gallon bucket. This took place at Bayer Industries in Houston, Texas. The second phase consisted of conducting laboratory tests to capture the density and unconfined compressive strength of the PF samples using ASTM D1621 and ASTM D1622 specifications. The laboratory tests were conducted by LTRC. Standard statistical testing methods comparing the control to the treatments were not conducted due to large differences between the control and the treatments, especially in wet conditions. In many instances, samples prepared in wet environments were so weak that their unconfined compressive strengths would have been less than “1 psi” at 3 percent strain. Because of that, only discussions of the average values were composed.

Phase 1

Injection Molds

In order to capture the density and unconfined compressive strength of PF in “free rise” conditions, injection molds were constructed with 3-in. diameter and 6-in. diameter PVC pipes. The height of the molds was approximately 4-in., as presented in Figure 21. *Free rise* is a term used to represent the properties of PF in conditions where PF is allowed to expand and cure without vertical confinement under dry conditions [1-6]. The walls of the PVC pipe, though, do provide some horizontal confinement, which affects both the density and UCS of samples as test data will later show. It has been well documented that both the density and unconfined compressive strength should increase under three dimensional confined conditions (vertical and horizontal) as compared to the free rise conditions [1-6]. With that being the case, free rise specimens from the molds were used as the control for this experiment. Target PF densities were, 4 pcf, 6 pcf, 8 pcf, and 12 pcf under dry conditions. Injecting into a wet environment was not attempted with the molds, because the expanding PF simply pushes the water out of the molds during expansion.



Figure 21
PVC injection molds

55 Gallon Barrel Test

The purpose of this test was to simulate the effect of injecting PF into a large void where minimal horizontal and no vertical confinement was present under both wet and dry conditions and capture its properties, as presented in Figure 22. The procedure entails injecting approximately 9 lbs. of PF into the barrel and allowing it to expand uninhibited other the side containment from the barrel. Once the PF fully expanded, it was removed from the barrel as seen in Figure 23.



Figure 22
Barrel test



Figure 23
PF in barrel

Box Test

This test was intended to simulate conditions that may exist beneath the pavement. A box was constructed and covered with a metal plate, as shown in Figure 24. Four 55-gallon drums filled with liquid were then placed on top of the metal plate. PF was injected through the metal plate into the void (approximately 1.75 in. deep) and allowed to expand. Figure 25 presents the PF in the box once the metal plate has been removed. Once PF expansion occurred, samples were taken in accordance with ASTM D1621. This process was repeated with the void being filled with water. PF with free rise design densities of 4, 6, 8, and 12 pcf were tested.



Figure 24
Box test



Figure 25
Expanded PF in box

Sand Bucket Test

The purpose of this test was to discover the properties of the sand/PF mixture and demonstrate how PF mixes with sand while expanding. A five gallon bucket was filled to 0.75 percent of its capacity with sand. PF was injected into the bottom of the bucket and allowed to expand, as presented in Figure 26.



Figure 26
Sand bucket test

Phase 2

Laboratory Testing Results for Injection Mold Samples

Samples were obtained from the 3-in. and 6-in. injection molds and subjected to visual inspection, density testing (ASTM D1622) and unconfined compression testing (ASTM D1621). Figure 27 presents the sample specimens from the 3-in. and 6-in. diameter molds.

Based upon the visual inspection of the specimens, it was clear that the PF split and cracked during its expansion in the 6-in. diameter mold while the PF sample in the 3-in. mold remained intact. According to Scott Brown of Bayer Industries, once the mold diameter exceeds 3 in., fracturing and tearing will occur in the specimens, and this experiment proved that point. For that reason, only specimens from the 3-in. diameter molds were used for density and unconfined compression testing.



Figure 27
Specimens from 6-in. and 3-in. diameter molds

Density tests were conducted in accordance with ASTM D1621 and the results are presented in Table 12. The target densities and measured densities differed with the measured densities being larger. This was an important discovery since the density of PF and its expansion rate are related as presented in Figure 3 and Table 1. Higher density PF has less expansion and therefore requires higher quantities to fill voids or lift slabs. For that reason, density and strength ranges are part of DOTD’s specification for PF with penalties, as presented in Appendix 2.

Table 12
Density and UCS results from 3-in. mold specimens

Target "Free rise" Polyurethane Foam Density	4 pcf		6 pcf		8 pcf		12 pcf	
3 in. Mold (wet or dry)	dry		dry		dry		dry	
Parameter	UCS	Density	UCS	Density	UCS	Density	UCS	Density
Unit	psi	pcf	psi	pcf	psi	pcf	psi	pcf
Max.	71.4	4.6	125.9	6.5	240.5	11.7	445.5	15.3
Min.	48.8	4.6	101.8	6.3	116.7	10.0	289.9	14.7
AVG.	65.0	4.6	113.3	6.5	181.3	10.5	392.5	14.9
STDEV.	8.2	0.0	8.7	0.1	39.0	0.5	59.6	0.2
Number of samples	6	6	8	10	10	10	10	10

Note: USC @ 3 % strain

Unconfined compression tests were conducted with the United testing machine in accordance with ASTM D1622 specifications. Figures 28 and 29 present an image of the United testing machine and load versus extension curves for a soil cement specimen and PF specimen. Normally, the load at three percent strain was used to determine the UCS of soil cement as

presented in Figure 29. Because of that, the load at three percent strain was also used to determine the UCS of the free rise PF as well. As presented in Table 12, the UCS for 4-, 6-, 8-, and 12-pcf were 65-, 113-, 181-, and 393-psi, respectively. As the density of PF increases so should the UCS, which this experiment has demonstrated. When comparing the UCS of PF with typical UCS design values of soil cement (300 psi) in Louisiana, all UCS values for PF fall below that value.



Figure 28
United testing machine

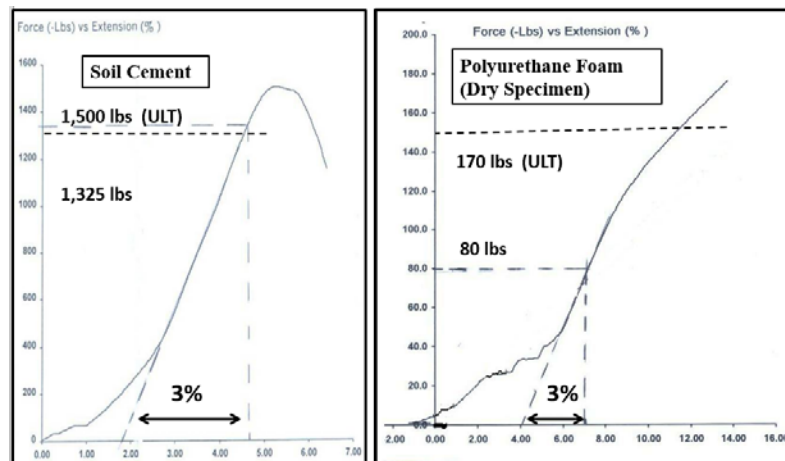


Figure 29
Load versus extension graphs

Laboratory Testing for Barrel Specimens

Samples were obtained from the barrel and subjected to visual inspection, density testing (ASTM D1621), and unconfined compression testing (ASTM D1622). Figure 30 presents a sample from one of the barrel tests. Visual inspection of the sample indicated that severe

tearing and fracturing occurred during the PF expansion process. Tearing and fracturing of PF during its expansion process in “unconfined” environments is normal, according to Scott Brown of Bayer Industries. Because of that, obtaining random specimens from the samples were not possible, so specimens were obtained from locations that appeared intact, which means the results are biased.



Figure 30
Specimens from barrel test

Specimens were obtained from the sample by using a drill and coring device as presented in Figure 31. The cored samples and specimens are presented in Figures 32 and 33. For the barrel test, specimens were available from wet and dry conditions for the densities of 4 and 6 pcf. Dry condition testing only was conducted for the PF densities of 4, 6, 8, and 12 pcf. The specimens obtained met ASTM D1622 standards.



Figure 31
Drill and coring device



Figure 32
Cored barrel sample

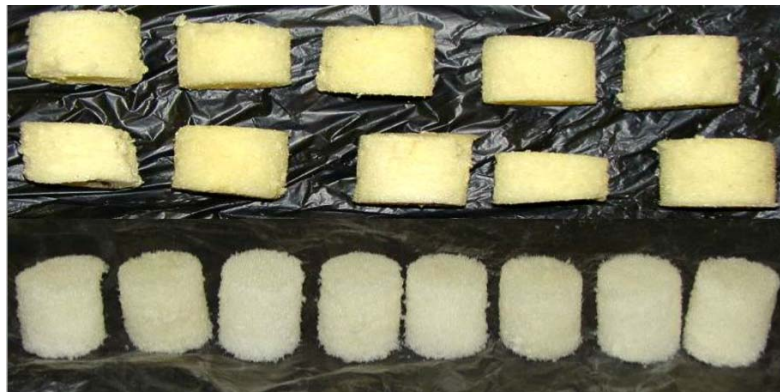


Figure 33
Specimens from barrel test

Density and UCS testing results are presented in Table 13. It should be noted that the UCS values reported in Table 13 are at ultimate load, not three percent strain. The authors reported it in this way due to the very low strengths measured during tests. Discussion on each test follows.

4 PCF PF Dry and Wet Specimens. The measured average density for free rise specimens was 4.6 pcf (Table 12) and the average measured densities from the dry and wet specimens were 2 and 13.2 pcf, respectively. It is unknown why the average dry density from barrel samples was much lower than the densities from the free rise specimens, but the authors postulate that it is due to minimal horizontal confinement from the barrel test. So in essence, the barrel test is nearer to true free rise conditions than the 3-in. molds. The authors postulate that the densities in the wet specimens were much larger than the free rise specimens because water was occupying void spaces within the PF as they would in a sponge.

The measured average free rise UCS was 65 psi while the average measured UCS from the dry and wet specimens were 5.5- and 2.0-psi, respectively. Both dry and wet UCS strengths were significantly lower than their free rise UCS counterparts. The reason(s) for this is unknown to the authors.

6 PCF PF Dry and Wet Specimens. The measured average density for free rise specimens was 6.5 pcf (Table 12) and the average measured densities from the dry and wet specimens were 2.1- and 25.2- pcf, respectively. As with the 4 pcf specimens, the dry density from barrel samples were much lower than the densities from the free rise specimens. Similar to the 4 pcf specimens, the densities in the wet specimens were much larger than the free rise specimens because the authors postulate that water was occupying void spaces within the PF as they would in a sponge.

The measured average free rise UCS was 113.3 psi while the average measured UCS from the dry and wet specimens were 1.9- and 2.3-psi, respectively. Both dry and wet UCS strengths were significantly different from their free rise UCS, a trend similar to the 4 pcf specimens. The UCS strengths for the 6 pcf specimens were either similar to or less than the strengths for the 4 pcf specimens, while they should have been consistently larger. The reason for this remains unknown to the authors.

8 PCF PF Dry Specimens. The measured average density for free rise specimens was 10.5 pcf (Table 12) and the average measured density from the dry specimens were 2.6 pcf. As with the 4- and 6-pcf specimens, the dry density from barrel samples were much lower than the densities from the free rise specimens.

The measured average free rise UCS was 181.3 psi while the average measured UCS from the dry specimens was 9.2 psi, respectively. The dry UCS strength was significantly lower than the free rise UCS; a trend similar to the 4- and 6-pcf specimens.

12 PCF PF Dry Specimens. The measured average density for free rise specimens was 14.9 pcf (Table 12) and the average measured density from the dry specimens was 4.1 pcf. As with the 4-, 6-, and 8-pcf specimens, the dry density from barrel samples were much lower than the densities from the free rise specimens.

The measured average free rise UCS was 392.5 psi while the average measured UCS from the dry specimens was 4.1 psi, respectively. The dry UCS strength was significantly lower than the free rise UCS, a trend similar to the 4-, 6-, and 8-pcf specimens.

**Table 13
Density and UCS results for barrel test**

Target "Free rise" Polyurethane Foam Density	4 pcf		4 pcf		6 pcf		6 pcf	
Barrel (wet or dry)	DRY		WET		WET		DRY	
Parameter	UCS	Density	UCS	Density	UCS	Density	UCS	Density
Unit	psi	pcf	psi	pcf	psi	pcf	psi	pcf
Max.	7.1	2.8	2.5	31.6	4.5	41.0	2.8	6.6
Min.	4.0	1.8	1.5	1.6	1.1	3.3	1.0	1.3
AVG.	5.5	2.0	2.0	13.2	2.3	25.2	1.9	2.1
STDEV.	1.1	0.3	0.3	13.9	1.1	14.1	0.6	1.6
Number of samples	10	10	11	11	7	7	10	10
Target "Free rise" Polyurethane Foam Density	8 pcf		12 pcf					
Barrel (wet or dry)	DRY		DRY					
Parameter	UCS	Density	UCS	Density				
Unit	psi	pcf	psi	pcf				
Max.	12.9	3.0	9.6	4.3				
Min.	6.3	2.2	1.8	1.4				
AVG.	9.2	2.6	4.1	2.5				
STDEV.	2.4	0.2	2.5	1.1				
Number of samples	10	10	11	11				

Note: UCS at ultimate load

Laboratory Testing for Box Specimens

As with the barrel test, samples were obtained from the boxes and subjected to visual inspection, density testing (ASTM D1621), and unconfined compression testing (ASTM D1622). Figure 34 presents a sample from one of the box tests. Visual inspection of the samples indicated that the samples were intact during the PF expansion process for both wet and dry conditions, unlike with the barrel test. Because of that, it was possible to obtain random specimens from the samples.



Figure 34
Samples from box test

Density and UCS testing results are presented in Table 14. It should be noted that the UCS values reported in Table 14 are at ultimate load, not three percent strain. The authors reported it in this way due to the very low strengths measured during tests. Discussion on each test follows.

4 PCF PF Wet Specimens. The measured average density for free rise specimens was 4.6 pcf (Table 12) and the average measured densities from the wet specimens were 4.6 pcf. Unlike the specimens from the barrel tests, the average wet density from the box sample was similar to the average density from the free rise specimens.

The measured average free rise UCS was 65 psi while the average measured UCS from the wet specimens 4.3-psi. The average wet UCS strengths were significantly lower than free rise UCS. The reason(s) for this is unknown to the authors.

6 PCF PF Dry and Wet Specimens. The measured average density for free rise specimens was 6.5 pcf (Table 12) and the average measured densities from the dry and wet specimens were 6.7 and 2.6 pcf, respectively. As with the 4 pcf specimens, the average dry density from the box samples were similar to the densities from the free rise specimens. However, the average densities in the wet specimens were much smaller than in the free rise specimens.

The measured average free rise UCS was 113 psi while the average measured UCS from the dry and wet specimens were 71.1 and 5.1 psi, respectively. Both dry and wet UCS strengths were significantly lower than their average free rise UCS. The reason(s) for this is unknown to the authors.

8 PCF PF Dry and Wet Specimens. The measured average density for free rise specimens was 10.5 pcf (Table 12) and the average measured densities from the dry and wet specimens were 10.2 and 3.3 pcf, respectively. The average dry density from the box samples was similar to the average density from the free rise specimens while the average wet density was significantly lower.

The measured average free rise UCS was 181.3 psi while the average measured UCS from the dry and wet specimens were 194.3 and 4.0 pcf, respectively. The average dry UCS strength was slightly larger than the average free rise UCS and the average wet UCS was much smaller.

12 PCF PF Dry and Wet Specimens. The measured average density for free rise specimens was 14.9 pcf (Table 12) and the average measured densities from the dry and wet specimens were 13.7 and 4.2 pcf, respectively. The average dry density from the box samples was near to the average density from the free rise specimens while the average wet density was significantly lower.

The measured average free rise UCS was 392.5 psi while the average measured UCS from the dry and wet specimens were 311.2 and 6.4 psi, respectively. The average dry UCS strength was close to the free rise UCS while the average wet UCS was significantly smaller.

Table 14
UCS and density test results from box test

Target "Free rise" Polyurethane Foam Density	4 pcf		6 pcf		6 pcf			
Box (wet or dry)	wet		wet		dry			
Parameter	UCS	Density	UCS	Density	UCS	Density		
Unit	psi	pcf	psi	pcf	psi	pcf		
Max.	4.7	5.9	8.9	3.7	81.1	8.3		
Min.	4.1	3.5	2.8	1.9	60.0	6.2		
AVG.	4.3	4.6	5.1	2.6	71.1	6.7		
STDEV.	0.2	0.9	1.5	0.5	8.6	0.7		
Number of samples	6	6	10	10	7	7		
Target "Free rise" Polyurethane Foam Density	8 pcf		8 pcf		12 pcf		12 pcf	
Box (wet or dry)	wet		dry		wet		dry	
Parameter	UCS	Density	UCS	Density	UCS	Density	UCS	Density
Unit	psi	pcf	psi	pcf	psi	pcf	psi	pcf
Max.	10.2	2.7	207.3	10.6	14.9	8.2	357.3	14.0
Min.	2.5	2.1	154.7	9.4	2.4	2.7	232.9	13.5
AVG.	4.0	3.3	194.3	10.2	6.4	4.2	311.2	13.7
STDEV.	2.2	1.0	19.7	0.4	3.7	1.9	41.3	0.2
Number of samples	11	11	6	6	8	8	8	8
Note: UCS at ultimate load								

Laboratory Testing for Sand Bucket Specimens

After PF was injected into the sand and allowed to expand, the sand/PF mixture was removed from the bucket, as shown in Figure 35. The sample was cored using a drill and 2-in. diameter core barrel to obtain specimens, as presented in Figures 36 - 38. All four specimens had some tearing and fracturing within them as presented in Figure 37. The sand/PF mixture was heterogeneous throughout the specimens. As presented in Figure 38, approximately 1- to 2-in. of the top and bottom of the specimen were a composite of sand/PF while approximately 3- to 4-in. of the mid region of the specimen was predominately PF, indicating that uniform mixing of sand and PF did not occur during the PF expansion process.



Figure 35
Sand/PF sample



Figure 36
Coring sand/PF bucket sample



Figure 37
Sand/PF specimens

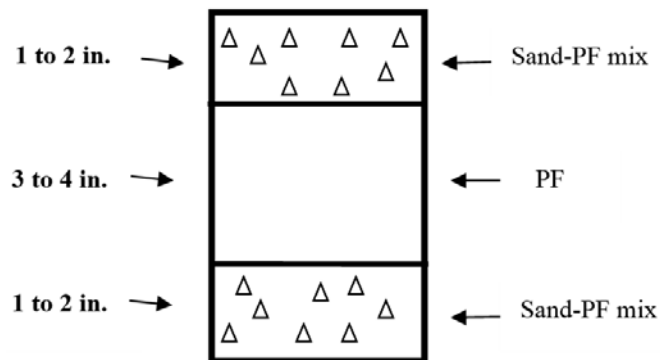


Figure 38
Diagram of sand/PF mixture

Density and UCS testing was conducted in accordance with ASTM D1621 and D1622 with the results presented in Table 15. Six pcf PF was injected into the sand bucket and the sand/PF mixture had an average density of 13.2 pcf. UCS test results indicated that the sand/PF mixture had an average UCS strength of 35 psi, which was significantly lower than the 113 psi UCS value from free rise samples.

Table 15
UCS and density results for sand/PF mixture

Target "Free rise" Polyurethane Foam Density	6 pcf	
Sand bucket (wet or dry)	dry	
Parameter	UCS	Density
Unit	psi	pcf
Max.	39.8	20.3
Min.	27.1	6.4
AVG.	35.0	13.2
STDEV.	6.9	5.7
Number of samples	3	4
Note: UCS @ 3 % strain		

Groupings of Test Data

Data were grouped from varying tests and densities in order to provide an overall snapshot of the test results. Beginning with the UCS strengths from molds, box test, sand bucket test, and barrel tests, it was obvious that UCS strengths from the mold specimens exceeded the UCS strengths from the box, barrel and sand bucket test as presented in Figure 39. This implies that if samples were procured from field tests where dry conditions were present, the UCS strengths would be less than in free rise conditions, which the 3-in. diameter molds were postulated to simulate. Regarding density relationships, with the exception of the sand bucket test, densities from the box and barrel tests were generally less than densities from the mold specimens. The results from the testing implies that when confining environments exist both the UCS and density are not increased as originally hypothesized.

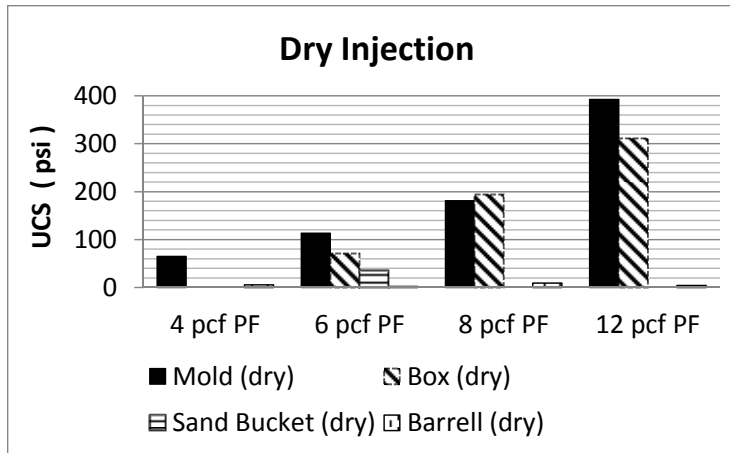


Figure 39
UCS dry injection sample comparison

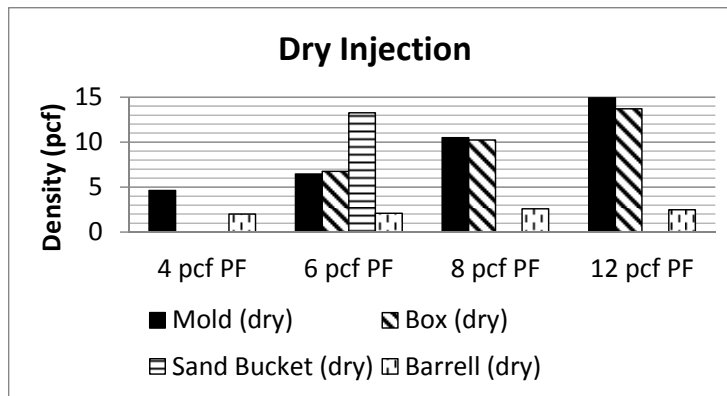


Figure 40
Density dry injection sample comparison

Figures 41 and 42 present the UCS and density results from barrel and box tests when water was present. The UCS strength was higher in the box test than the barrel test at the PF densities of 4, 6, and 12 pcf. Extremely weak UCS strengths were present in all tests. The measured densities from the box tests were larger than the measured densities from the barrel tests. The results of testing from the wet environments indicate that the hydrophobic Uretek 486 used in this experiment was extremely sensitive to water as evidenced from the UCS tests.

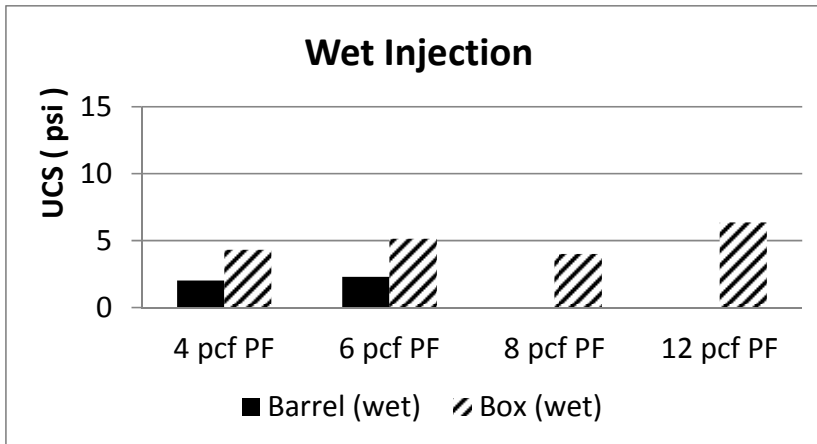


Figure 41
UCS wet injection sample comparison

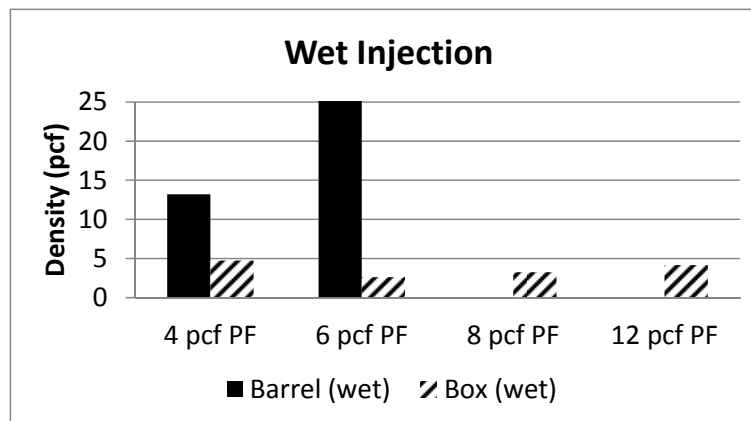


Figure 42
Density wet injection sample comparison

Figures 43 and 44 present comparisons between samples for the molds (dry injection) to samples from the box and barrel when water was present. The UCS strengths from the wet samples were extremely weak when compared to the samples from the molds. The UCS strengths from wet specimens ranged from about 2 to 9 psi implying that wet environments do not allow PF to gain much strength as presented in Figure 43. PF densities ranged from about 2 to 5 pcf when injected into wet environments indicating extreme sensitivity to water, as presented in Figure 44.

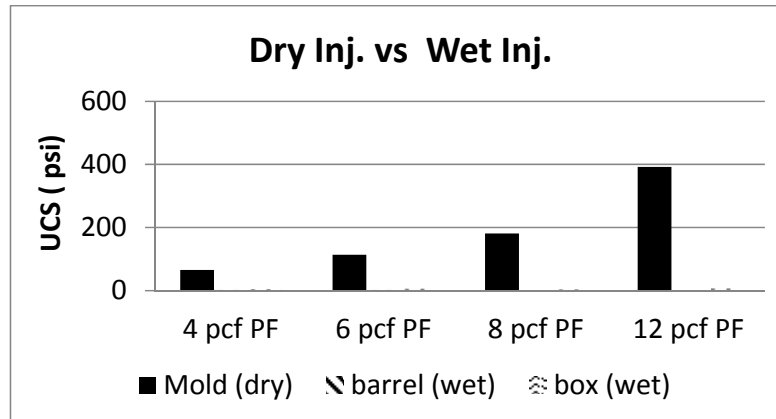


Figure 43
UCS wet injection versus dry injection sample comparison

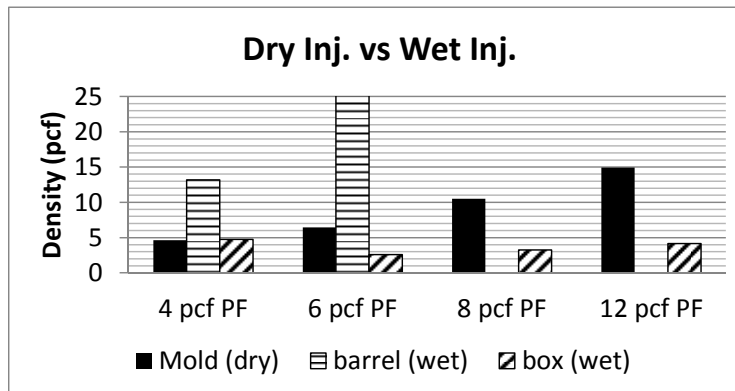


Figure 44
Density wet injection versus dry injection sample comparison

Highlights From Experimental Program

1. 3-in. diameter molds provide confinement to PF samples, which positively influences its properties. Molds with 3-in. diameters should be used to capture the properties of PF for quality control and pay purposes.
2. 55 gallon barrels provide a better environment to capture the unconfined or free rise properties of PF, but the sampling will be biased due to severe tearing and fracturing of PF during its expansion and curing process.
3. When PF is injected into an environment where water is present, its density and strength will be severely impacted to the point of offering little support.
4. When PF is injected into environments intended to simulate field conditions, both its density and UCS generally will be less than the densities and UCS obtained from samples prepared in 3 in. molds (free rise conditions).

5. PF does not mix uniformly with granular materials such as sand. When compared to free rise conditions, the density of a PF-granular-material-mixture increases while it's UCS is significantly less, depending upon where the specimen is taken.
6. The high variability in PF densities and UCS obtained from the different test environments warrant extreme caution. Very conservative design considerations should be employed when using this material.

APPENDIX 2: SPECIFICATIONS

DESIGN ENGINEER INSTRUCTIONS

***DO NOT USE WITHOUT FHWA INDIVIDUAL PROJECT AUTHORIZATION.
CONTACT THE SPECIFICATIONS UNIT FOR ADDITIONAL INSTUCTIONS.***

NS RAISING AND/OR UNDER-SEALING CONCRETE SLABS (POLYURETHANE) (03/10): (STATE PROJECT NO. _____) (FHWA AUTHORIZATION REQUIRED)

DESCRIPTION. This item consists of raising and/or under-sealing concrete slabs by an approved method using a high-density hydrophobic polyurethane foam (PF) at the locations shown on the plans, as described herein, as directed by the engineer, and in accordance with the manufacturer's recommendations. Hydrophobic means that the PF shall lose no more than 10 percent of its density or strength when injected into liquid water. This work includes drilling injection holes, installation of injection tubes directly below the slab or to a depth not to exceed six inches (0.15m) from the bottom of the concrete slab, if needed to raise the slab, injecting material to underseal the concrete slab, checking elevations to control lift of pavement, filling and sealing injection holes, cleanup, and other related work.

MATERIAL. The material used for raising and/or under-sealing concrete slabs shall be a high-density hydrophobic polyurethane foam, as approved by the engineer, having a water insoluble diluent that permits the formation of polyurethanes in excess water. The material shall have a free rise density ranging from 3.0 to 4.0 pounds per cubic foot (48.1 to 64.1 kg/m³) and a minimum average unconfined compressive strength of 50 psi.

Material Specifications and Material Safety Data Sheets (MSDS): The contractor shall submit a manufacturer's materials specification and MSDS sheet defining the typical resin properties, general description of material, mix ratio, typical reaction properties, typical physical properties, ingredients hazard classification, physical data, fire and explosion hazard data, and reactivity data. The formula and characteristics shall be certified by the manufacturer and verified in the field.

Prior to beginning work, 5 machine mixed field samples will be prepared by the contractor in 4-in. diameter molds approximately 4 in. tall in accordance with ASTM D1621. The samples shall then be taken to an approved laboratory at the contractor's expense and a 2-in. by 2-in. by 2-in. (50 mm by 50 mm by 50 mm) sample shall be taken from the center of the 4 in. (100 mm) diameter molded sample and an unconfined compressive strength shall be determined in accordance with ASTM D1621. The density of the material shall be determined from the

specimen group used for unconfined compressive strength tests in accordance with ASTM D1622. The unconfined compressive strength and density determined from ASTM D1621 and ASTM D1622 shall be used to determine the percent of pay for this item as outlined in Measurement and Pay. The contractor shall submit electronic copies of the stress strain curves (ASTM D1621){Force (lbs) vs. Extension(%)} and density calculations including measured specimen dimensions (ASTM D1622) for each specimen tested to the engineer. Field testing will be required for every 25,000 pounds of material used on the project or at the engineer's discretion.

WARRANTY. Manufacturer shall warrant the product performance for five years from final acceptance. Manufacturer shall be responsible for all costs associated with repair or replacement.

EQUIPMENT. The following list of under-sealing equipment shall be considered the minimum amount of equipment to perform the work.

- (a) A drill capable of drilling 5/8-in. (16 mm) diameter holes shall be provided and, when directed injection tubing installed to a depth not to exceed 6 in. (150 mm) from the bottom of the concrete slab.
- (b) A pumping unit capable of injecting the polyurethane material to the depth required under the pavement and capable of controlling the rate of rise of the pavement. Pumping units shall be equipped with a manufacturer's certified flow meter to measure the amount of chemical injected. The certified flow meter shall have a digital output in both pounds (kg) and gallons (liters). Polyurethane material will be measured to the nearest pound (kg) as displayed by the certified flow meter.
- (c) A laser leveling unit to ensure that the concrete pavement is raised to an even plane or to the required elevation.

CONSTRUCTION REQUIREMENTS:

Drilling and Injecting: A series of 5/8-in. (16 mm) diameter holes shall be drilled at approximately 6-ft. (2-m) intervals maximum through the concrete in the area to be raised and/or under-sealed. The exact location and spacing of the holes shall be determined by the contractor and be approved by the engineer. A high-density polyurethane formulation shall be injected under the slab to a maximum depth not to exceed 6 in. (150 mm) beneath the concrete slab, only if needed to raise the slab. The pumping unit shall control the amount of rise by regulating the rate of injection of the polyurethane material. The finished concrete slab shall conform to the grade and cross-section of the slab prior to settlement. Elevations shall be within a tolerance of +/- 1/4-in. of the required grades or as much as the slab allows, at

the direction of the engineer. When the nozzle is removed from the hole, any excessive polyurethane material shall be removed from the area and the hole sealed for the full depth of the concrete pavement with an approved cementitious grout. If the engineer determines that the base is too wet, polyurethane injection will be postponed until conditions improve.

The contractor shall be responsible for any pavement blowouts, cracking, excessive lifting, or uneven pavement that results from raising and/or under-sealing of the pavement. Any damage to the pavement occurring prior to final acceptance shall be repaired by the contractor as directed at no direct pay.

Set-Time: The high-density polyurethane formulation used shall set and obtain at least 90 percent of its ultimate compressive strength within 15 minutes after final injection.

MEASUREMENT AND PAYMENT. Polyurethane material will be measured to the nearest pound (kg) as displayed by the certified flowmeter. Under-sealing Concrete Slabs will be measured and paid for at the adjusted contract unit price per pound (kg) of high-density polyurethane material injected, including all materials, tools, equipment, labor, warranty, and incidentals necessary to complete the item. Payment per pound (kg) shall be determined and/or adjusted as follows:

Payment Adjustment for Density and Unconfined Compressive Strength ¹

Density, lb/cu.ft.	< 3.0	3.0 to 4.0	> 4.0
% Pay	No pay	100	(See formula Below) ²
Unconfined Compressive Strength, psi	< 50	≥ 50	≥ 50
% Pay	No pay	100	100

¹ The total payment will be the lowest of the percent payments for density and compressive strength per 25,000 lb test batch.

² The adjustment in pay for density shall be applied to the pounds of material used as based on the unit price of the polyurethane material indicated on the manufacturer's invoice.

Percent Pay = (4.0 / Density) * 100

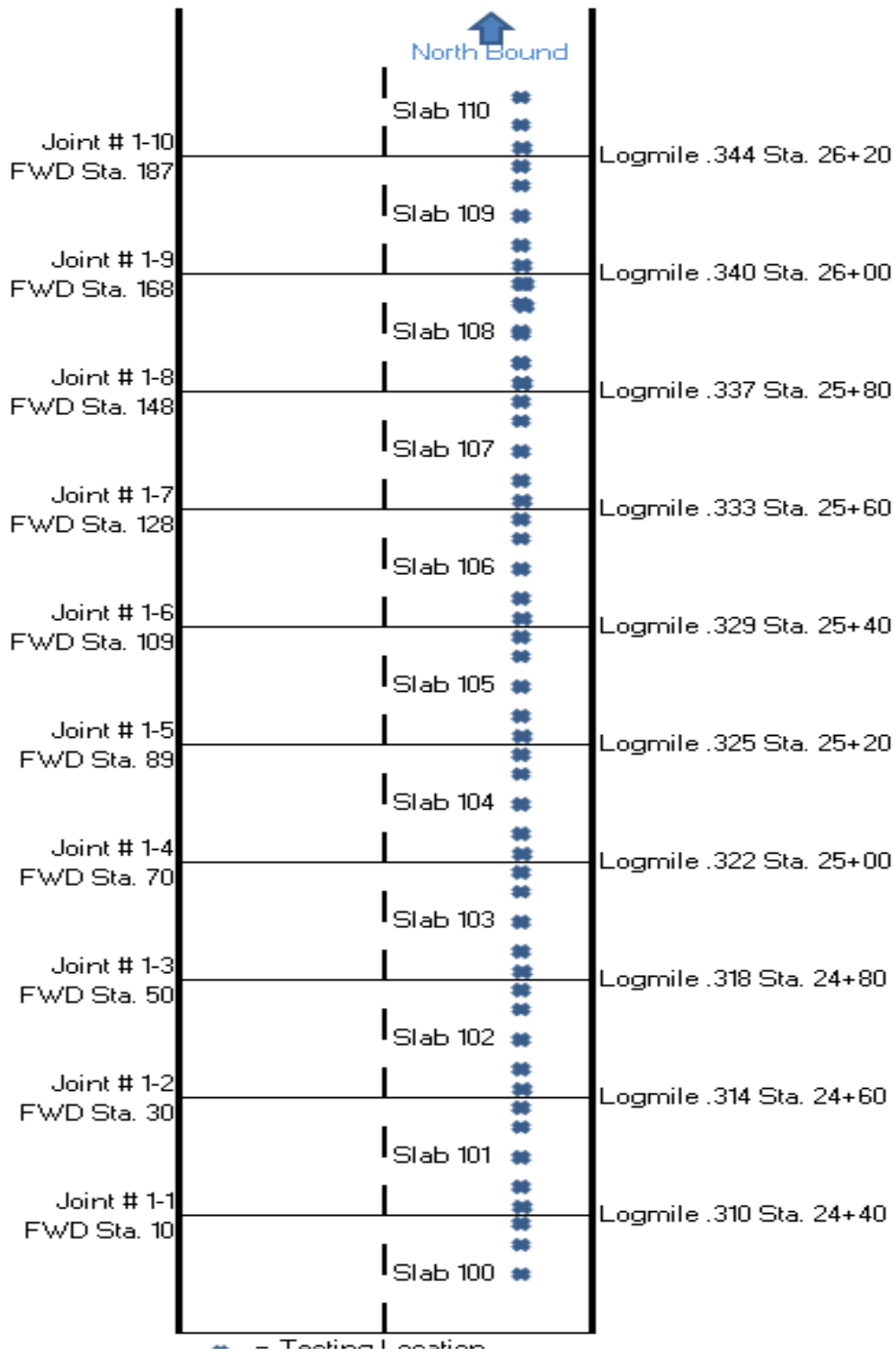
Density = average density (lb/cu.ft) per 25,000 lb batch per ASTM 1622 (round to 1 decimal place)

Payment will be made under:

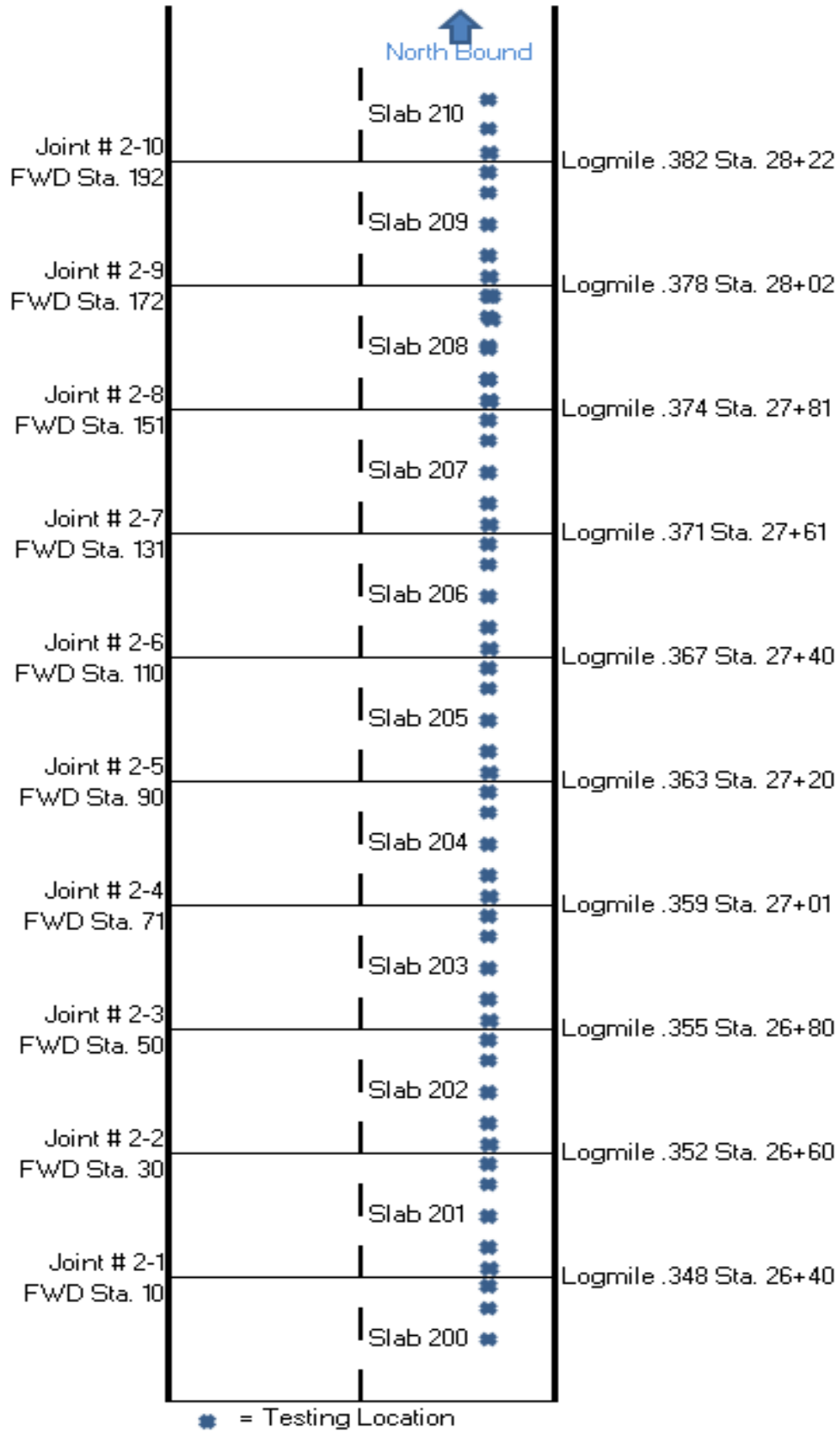
<u>Item No.</u>	<u>Pay Item</u>	<u>Pay Unit</u>
NS-602-00003	Raising and/or Under-Sealing Concrete Slabs (Polyurethane)	Pound
(kg)		

APPENDIX 3: TEST SECTION LAYOUT

LA 1 Uretek Project Section 1



LA 1 Uretek Project Section 2



LA 1 Uretek Project Section 3

